NHC Complexes of Osmium Clusters: A Structural and Reactivity Study

Craig E. Cooke,*,† Michael C. Jennings,‡ Michael J. Katz,§ R. K. Pomeroy,§ and Jason A. C. Clyburne*,†

Department of Chemistry, Saint Mary's University, Halifax NS B3H 3C3, Canada, Department of Chemistry, University of Western Ontario, 1151 Richmond Street, London ON N6A 5B7, Canada, and Department of Chemistry, Simon Fraser University, 8888 University Drive, Burnaby BC V5A 1S6, Canada

Received June 23, 2008

A carbene transfer agent, 1,3-bis-(2,4,6-trimethylphenyl)imidazol-2-ylidene-silver(I)chloride ([IMes]-AgCl), was treated with various osmium clusters. Reaction of ([IMes]AgCl) with $[Os_3(\mu\text{-H})_2(CO)_{10}]$ gave $[Os_3(\mu\text{-H})(\mu\text{-Cl})(CO)_9(IMes)]$ (**1**), an osmium *N*-heterocyclic carbene complex. The reaction of ([IMes]AgCl) with the cluster $[Os_3(CO)_{10}(CH_3CN)_2]$ yielded two products, $[Os_3(\mu\text{-Cl})(CO)_{10}(\mu\text{-Ag(IMes)}]$ (**2**) and [(IMes-H)]$[Os_3(\mu\text{-Cl})(CO)_{10}](\mu_4\text{-Ag})[Os_3(\mu\text{-Cl})(CO)_{10}]$ (**3**). Compound (**2**) is a heterobimetallic carbene complex resulting from the complete incorporation of ([IMes]AgCl). Transmetalation using [(IMes)AgCl] and the cluster $[Os_4(\mu\text{-H})_4(CO)_{12}]$ in the presence of trimethylamine-*N*-oxide resulted in the formation of $[Os_4(\mu\text{-H})_4(CO)_{11}(n\cdot\text{IMes})]$ (**4**), where (*n* denotes normal carbene bonding, i.e., through C_2). $[Os_4(\mu\text{-H})_4(CO)_{10}(IMes)_2]$ (**5**) was formed using the activated cluster $[Os_4(\mu\text{-H})_4(CO)_{10}(CH_3CN)_2]$ and [(IMes)AgCl]. Compound (**5**) was found to be sensitive to silica gel column chromatography in the presence of dichloromethane decomposing to $[Os_4(\mu\text{-H})_3(\mu\text{-Cl})(CO)_{11}(IMes)]$ (**6**), which possessed a butterfly metal skeleton. The ruthenium analogue of (**4**), $[Ru_4(\mu\text{-H})_4(CO)_{11}(IMes)]$ (**7**), was prepared and identified spectroscopically but was found to be thermally unstable. Thermolysis of (**4**) in benzene yielded four products. The abnormal carbene complex $[Os_4(\mu\text{-H})_4(CO)_{11}(a\cdot\text{IMes})]$ (**10**) (*a* denotes abnormal carbene bonding through C_3 or C_4), an isomer of (**4**), and $\{Os_4(\mu\text{-H})(CO)_{10}[(\eta\text{-C})N(Mes)C_2H_2NC_6H_2(CH_3)_2(\eta^2\text{-C})(\eta\text{-C})C_4H_4(\eta^2\text{-C})]\}$ (**11**), an unusual complex resulting from the activation of benzene and activation of three C−H bonds on IMes, were isolated in modest yields. Two higher-nuclearity clusters, $\{Os_5(\mu_5\text{-C})(CO)_{14}[\eta\text{-C-}\eta\text{-NC}_2H_2(Mes)]\}$ (**8**) and $[Os_6(\mu\text{-H})_4(\mu_5\text{-C})(CO)_{15}(IMes)]$ (**9**), both of which contain carbide ligands, were also isolated. $\{Os_4(\mu\text{-H})(CO)_{10}[(\eta\text{-C})N(Mes)C_2H_2NC_6H_2(CH_3)_2(\eta^2\text{-C})(\eta\text{-C})CHC(CH_3)\text{-}C_2\ H_2(\eta^2\text{-C})]\}$ (**12**), an analogue of (**10**), resulted from the thermolysis of (**4**) in toluene indicates that the reaction is potentially general and exhibits some regioselectivity. Crystal structure determinations were completed on all 11 osmium cluster complexes.

Introduction

The investigation of cluster compounds containing hydride ligands has long been of interest to chemists. The chemistry of hydrogen, specifically relating to its desired use as an energy source, has led to the increased interest in polynuclear metal complexes, which can take up and release hydrogen under mild conditions.[1] Materials of this nature are of interest for hydrogenation catalysts and hydrogen storage, particularly if the complexes can reversibly absorb large amounts of hydrogen.[1] Osmium and ruthenium carbonyl clusters are able to undergo hydrogenation via displacement carbonyl ligands affording clusters with varied metal and hydride numbers. As expected, these materials exhibit reactivities that are different from their corresponding binary carbonyls, in many cases providing stable complexes.

Carbenes are neutral compounds featuring a divalent carbon atom with only four electrons in its valence shell. Complexes prepared from the metalation of imidazolium-2-ylidene, better known as *N*-heterocyclic carbenes (NHCs), have the general structure shown in Figure 1. NHCs have also been prepared, which contain a variety of heteroatoms other than nitrogen (such as C, B, O, etc.) within in the ring.[2] The use of NHCs as ligands for transition metals was first described in 1968 by Öfele and Wanzlick.[3,4] Aside from the pioneering work of Lappert on transition metal−carbene complexes, few papers on this topic

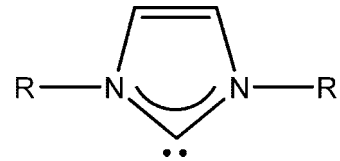

Figure 1. Generalized formula of an *N*-heterocyclic carbene where R is an organic moiety.

* Corresponding author. E-mail: Jason.Clyburne@SMU.CA.
† Saint Mary's University.
‡ University of Western Ontario.
§ Simon Fraser University.

(1) Adams, R. D.; Captain, B. *Angew. Chem., Int. Ed.* **2008**, *47*, 252–257.

(2) Bertrand, G. *Carbene Chemistry: From Fleeting Intermediates to Powerful Reagents*; CRC Press: New York, 2002. (a) Prasäng, C.; Donnadieu, B.; Bertrand, G. *J. Am. Chem. Soc.* **2005**, *127*, 10182–10183. (b) Krahulic, K. E.; Enright, G. D.; Parvez, M.; Roesler, R. J. *J. Am. Chem. Soc.* **2005**, *127*, 4142–4143. (c) Canac, Y.; Soleilhavoup, M.; Conejero, S.; Bertrand, G. *J. Organomet. Chem.* **2004**, *689*, 3857–3865.

(3) Ofele, K. *J. Organomet. Chem.* **1968**, *12*, P42.

(4) Wanzlick, H. W.; Schoenherr, H. J. *Angew. Chem., Int. Ed. Engl.* **1968**, *7*, 141–142.

10.1021/om800577x CCC: $40.75
Publication on Web 10/22/2008

had been published prior to the early nineties.[5] However, following the isolation of the first NHC by Arduengo in 1991, research on metal−carbene complexes expanded greatly.[2,6−10] Free carbenes, as well as those in metal complexes, have been studied extensively.[2,6,7,11−13]

Complexes of NHCs have been prepared with virtually every transition metal and many main group elements, a consequence of the ability of NHCs to bind to both hard and soft metals making it a very versatile ligand system.[10,12] NHCs bond to metals primarily through σ-donation of the carbene lone pair to the metal. Carbene bonding was believed to have been purely σ-donation in nature; however, recent evidence suggests that some degree of back-donation may occur.[14−16] The extent of π-back-donation is dependent upon the metal center to which it is bound; it is believed to be smaller than that of Fischer carbenes.[16] The bond strength of *N*-heterocyclic carbenes has been shown to rival phosphines. Imidazolin-2-ylidene, the first type of NHC to be complexed to silver, is an imidazole ring with substituents at the nitrogen atoms (1,3-position) and with the singlet carbene located at the 2-position, and has the general structure shown in Figure 1.[8,11−13] The stability of NHC−metal complexes is due to the π-donation from the p-orbitals of the nitrogen atoms to the empty p-orbital of the carbon atom.[15,17]

NHCs and phosphines share the properities of both being monodentate two-electron ligands. NHCs provide a versatile alternative to phosphine ligands, often showing stronger electron-donating properties while also providing an equally variable steric environment.[8,11−13,18,19] This results in several advantages including tighter binding (which often limits catalyst decomposition reactions associated with ligand dissociation) and greater thermal stability than that observed for phosphines.[8,11−13,18] In tertiary phosphines, PR_3, a change of the substituent causes a change in both the steric and electronic environment of the ligand since the R group is bound directly to the phosphorus donor atom. NHCs, however, exhibit little change on variation of the nitrogen-bonded substituent as it is not directly attached to the donor atom. A change of *N*-bonded substituents primarily changes the steric nature of the NHC. It has been proposed that in order to affect an electronic change in an NHC ligand, it is best to modify the azole ring.[8,10,12,20−22]

The sterics of phosphines and NHCs are different; NHCs are fan-shaped and as such can orient themselves via rotation about the donor atom−metal bond to minimize steric interactions with other ligands. Phosphines, however, are usually cone-shaped, and rotation about the phosphorus−metal bound is not typically hindered. Extensive work with phosphines was completed in this regard by Tolman, who developed the concept of the cone angle.[12,20,23] To quantify the steric factors characterizing NHC ligands, Nolan suggests that the NHC shape can best be described as the volume of a sphere centered on the metal, buried by overlap with atoms of the various NHC ligands denoted by %VBuried.[24,25] The volume of this sphere represents the space around the metal atom that must be shared by the different ligands upon coordination. The bulkier a specific ligand, the larger the portion of the sphere that will be occupied by that ligand, i.e., the greater %VBuried.[16,24] The cone angle and %VBuried provide a structured approach to steric analysis. Given the different steric requirements of NHCs, it is expected that their reaction with clusters will result in a metal complex shrouded by the carbene when viewed as a space filling model, while PR_3 ligands are oriented away from the metal centers and thus are less likely to participate in intramolecular reactions.

A great deal of research has been completed examining the synthesis of NHC analogues of phosphine catalysts. As such, a large library of palladium and ruthenium complexes containing NHCs exists;[8,12,13,18,26,27] from these investigations, it was found that NHCs are often reactive within the coordination sphere, i.e., NHCs are noninnocent ligands.[13] Several reports illustrate that NHCs are susceptible to C−H activation on the *N*-substituents.[28−32] Also, reductive eliminations have been identified.[33,34] One of the most studied systems in this respect involves mononuclear iridium−NHC complexes.[28,29,31,35,36] This reactivity is quite different from that of tertiary phosphines, which are typically thought of as spectator ligands as they rarely undergo any modification during a reaction.[20]

Several research groups have investigated the use of NHC−silver(I) halide complexes as NHC transfer agents and have successfully prepared NHC complexes of several late transition metals by this method.[11,12] We choose to use the

(5) Cardin, D. J.; Cetinkaya, B.; Lappert, M. F. *Chem. Rev.* **1972**, *72*, 545–574.
(6) Arduengo, A. J., III; Harlow, R. L.; Kline, M. *J. Am. Chem. Soc.* **1991**, *113*, 361–363.
(7) Arduengo, A. J., III *Acc. Chem. Res.* **1999**, *32*, 913–921.
(8) Bourissou, D.; Guerret, O.; Gabbai, F. P.; Bertrand, G. *Chem. Rev.* **2000**, *100*, 39–91.
(9) Lee, K. M.; Wang, H. M. J.; Lin, I. J. B. *J. Chem. Soc., Dalton Trans.* **2002**, 2852–2856.
(10) Herrmann, W. A.; Schuetz, J.; Frey, G. D.; Herdtweck, E. *Organometallics* **2006**, *25*, 2437–2448.
(11) Lin, I. J. B.; Vasam, C. S. *Comments Inorg. Chem.* **2004**, *25*, 75–129.
(12) Garrison, J. C.; Youngs, W. J. *Chem. Rev.* **2005**, *105*, 3978–4008.
(13) Crudden, C. M.; Allen, D. P. *Coord. Chem. Rev.* **2004**, *248*, 2247–2273.
(14) Kelly, R. A., III; Clavier, H.; Giudice, S.; Scott, N. M.; Stevens, E. D.; Bordner, J.; Samardjiev, I.; Hoff, C. D.; Cavallo, L.; Nolan, S. P. *Organometallics* **2008**, *27*, 202–210.
(15) Khramov, D. M.; Lynch, V. M.; Bielawski, C. W. *Organometallics* **2007**, *26*, 6042–6049.
(16) Diez-Gonzalez, S.; Nolan, S. P. *Coord. Chem. Rev.* **2007**, *251*, 874–883.
(17) Sanderson, M. D.; Kamplain, J. W.; Bielawski, C. W. *J. Am. Chem. Soc.* **2006**, *128*, 16514–16515.
(18) Herrmann, W. A. *Angew. Chem., Int. Ed.* **2002**, *41*, 1290–1309.
(19) Sanderson, M. D.; Kamplain, J. W.; Bielawski, C. W. *J. Am. Chem. Soc.* **2006**, *128*, 16514–16515.
(20) Crabtree, R. H. *J. Organomet. Chem.* **2005**, *690*, 5451–5457.
(21) Fuerstner, A.; Alcarazo, M.; Krause, H.; Lehmann, C. W. *J. Am. Chem. Soc.* **2007**, *129*, 12676–12677.
(22) Chianese, A. R.; Li, X.; Janzen, M. C.; Faller, J. W.; Crabtree, R. H. *Organometallics* **2003**, *22*, 1663–1667.
(23) Tolman, C. A. *Chem. Rev.* **1977**, *77*, 313–348.
(24) Cavallo, L.; Correa, A.; Costabile, C.; Jacobsen, H. *J. Organomet. Chem.* **2005**, *690*, 5407–5413.
(25) Viciu, M. S.; Navarro, O.; Germaneau, R. F.; Kelly, R. A. III; Sommer, W.; Marion, N.; Stevens, E. D.; Cavallo, L.; Nolan, S. P. *Organometallics* **2004**, *23*, 1629–1635.
(26) Marion, N.; Diez-Gonzalez, S.; Nolan, S. P. *Angew. Chem., Int. Ed.* **2007**, *46*, 2988–3000.
(27) Scott, N. M.; Nolan, S. P. *Eur. J. Inorg. Chem.* **2005**, 1815–1828.
(28) Scott, N. M.; Pons, V.; Stevens, E. D.; Heinekey, D. M.; Nolan, S. P. *Angew. Chem., Int. Ed.* **2005**, *44*, 2512–2515.
(29) Scott, N. M.; Dorta, R.; Stevens, E. D.; Correa, A.; Cavallo, L.; Nolan, S. P. *J. Am. Chem. Soc.* **2005**, *127*, 3516–3526.
(30) Cabeza, J. A.; del Rio, I.; Miguel, D.; Sanchez-Vega, M. G. *Chem. Commun.* **2005**, 3956–3958.
(31) Hanasaka, F.; Tanabe, Y.; Fujita, K.-I.; Yamaguchi, R. *Organometallics* **2006**, *25*, 826–831.
(32) Jazzar, R. F. R.; Macgregor, S. A.; Mahon, M. F.; Richards, S. P.; Whittlesey, M. K. *J. Am. Chem. Soc.* **2002**, *124*, 4944–4945.
(33) McGuinness, D. S.; Saendig, N.; Yates, B. F.; Cavell, K. J. *J. Am. Chem. Soc.* **2001**, *123*, 4029–4040.
(34) Graham, D. C.; Cavell, K. J.; Yates, B. F. *Dalton Trans.* **2006**, 1768–1775.
(35) Corberan, R.; Sanau, M.; Peris, E. *Organometallics* **2006**, *25*, 4002–4008.
(36) Corberan, R.; Sanau, M.; Peris, E. *J. Am. Chem. Soc.* **2006**, *128*, 3974–3979.

Scheme 1. Predicted Reactivity of the NHC−Ag-X Transfer Agent

$$\text{NHC-Ag-X} + \text{ML}_n \longrightarrow \text{NHC-ML}_n + \text{AgX}_{(s)}$$

NHC−silver(I) halide transfer methods to introduce NHCs into clusters as it appeared to be the most robust. It was considered that the reagents for *in situ* deprotonation of imidazolium salts to generate a free carbene may be reactive with the cluster, particularly the hydride containing species.

Osmium *N*-heterocyclic carbene complexes are rare.[37] A survey of those known reveals only a few mononuclear species.[38−40] Osmium cluster−NHC derivatives have only recently been reported[41−43] as having ruthenium derivatives.[41,44−47] The lack of research in this area is surprising since the role of phosphines in cluster chemistry has been well documented and thoroughly explored. A key feature of small clusters containing transition metals is the ability of the metal sites to react in concert. This has the effect of enhancing the reactivity over that which can be achieved with single-site metal complexes.[42] Following several recent studies showing that NHC−metal bonds are not inert (see above) and that NHCs are able to participate in various inter- and intramolecular reactions, it was anticipated that clusters could provide an ideal reactive class of molecule to study this reactivity. The chemistry of NHCs in metal hydride clusters has not been probed, and this was considered to be of potential interest to catalyst design, reactivity of hydrogen bound to metals, and NHC activation.

The results of the studies presented herein can be separated into three sections: (1) NHC−AgCl transfer chemistry, which does not result in the formation of the anticipated product. This chemistry highlights the pitfalls of using silver(I) chlorides as an NHC source. (2) Chemistry in which the NHC is transferred successfully producing new NHC−cluster complexes. (3) Reactivity involving the NHC−cluster complexes.

Results and Discussion

The introduction of free NHCs can be technically demanding because of their highly reactive nature. In order to get around the reactivity of free carbenes, a carbene transfer agent can be used. One of the most studied transfer agents of this type is an NHC−silver(I) halide complex.[9,11,12,48−51] Silver(I) NHC complexes with a singly coordinating anion are neutral, with silver linearly bound to both the carbene and the halide. These complexes are an attractive class of molecules with potential for direct transmetalation of the NHC ligand.[12] This reaction is accompanied by the thermodynamically favorable formation of solid silver(I) halide, which typically precipitates during the course of the reaction (Scheme 1).

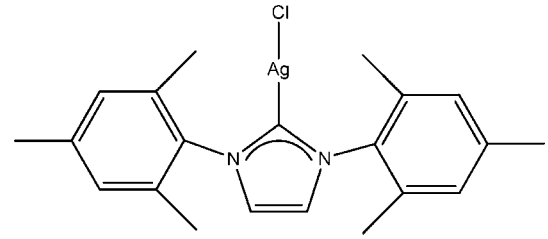

Figure 2. [(IMes)AgCl] (Mes = 2,4,6-trimethylphenyl), an NHC transfer complex used in this study, represented as a simple diagram.

The use of NHC silver(I) halides was considered to attempt the introduction of an NHC. As they are air- and moisture-stable allowing for convenient handling, these reagents allow for an easy starting point into the area of NHC−metal cluster chemistry.[12,51]

The NHC transfer complex used in this study is 1,3-bis-(2,4,6-trimethylphenyl)imidazol-2-ylidene-silver(I) chloride (Figure 2).[49] This NHC was chosen as it is simple to prepare, and examples detailing its activity have been shown with other systems. Other methods that can be used to introduce carbenes onto metals, aside from the use of free carbenes, include the use of imidazole salts, which are deprotonated *in situ*, the use of basic groups on the reactive metal center to induce deprotonation while freeing a site for coordination, and the use of electron rich olefins.[37]

1. Unusual NHC−AgCl Transfer Chemistry. Initial studies using [(IMes)AgCl] were considered with the simplest triosmium cluster species including $[Os_3(\mu\text{-H})_2(CO)_{10}]$ and $[Os_3(CO)_{10}(CH_3CN)_2]$. Selection of these molecules was based upon their unsaturated character and propensity toward facile ligand introduction under mild temperatures. Also, with the simple metal framework, it was hoped that it would limit the formation of multiple products.

Characterization of $[Os_3(\mu\text{-H})(\mu\text{-Cl})(CO)_9(IMes)]$ (1). Scheme 2 outlines the reaction conditions and chemicals used in the generation of $[Os_3(\mu\text{-H})(\mu\text{-Cl})(CO)_9(IMes)]$ (**1**). Thermal activation was used to introduce the IMes ligand into the unsaturated hydride cluster. Recrystallization of (**1**) was accomplished from a concentrated toluene and hexanes solution at −20 °C.

IR solution studies on a hexanes solution of (**1**) indicated the presence of eight ν(CO) bands and were indicative of a new complex. For comparison, five IR ν(CO) bands are exhibited for the starting material, $[Os_3(\mu\text{-H})_2(CO)_{10}]$. ^{1}H and ^{13}C{^{1}H} NMR solutions in CD_2Cl_2 studies on the crystalline solid material (**1**) confirm the presence of an IMes ligand. The ^{1}H NMR resonances (6H) for IMes ortho-methyl groups appear at 2.10 ppm and 2.12 ppm. A third resonance in the methyl region (6H) at 2.36 ppm has been assigned to the *para*-CH_3 group present on the IMes ligand.^{1}H NMR studies also revealed a single resonance at −13.3 ppm; the accepted region for bridging hydrides ranges from about 0 ppm to −25 ppm.[52,53] This

(37) Arnold, P. L.; Pearson, S. *Coord. Chem. Rev.* **2007**, *251*, 596–609.
(38) Mondal, T. K.; Mathur, T.; Slawin, A. M. Z.; Woollins, J. D.; Sinha, C. *J. Organomet. Chem.* **2007**, *692*, 1472–1481.
(39) Bolano, T.; Castarlenas, R.; Esteruelas, M. A.; Onate, E. *Organometallics* **2007**, *26*, 2037–2041.
(40) Castarlenas, R.; Esteruelas, M. A.; Onate, E. *Organometallics* **2005**, *24*, 4343–4346.
(41) Cabeza, J. A.; del Rio, I.; Miguel, D.; Perez-Carreno, E.; Sanchez-Vega, M. G. *Organometallics* **2008**, *27*, 211–217.
(42) Cooke, C. E.; Jennings, M. C.; Pomeroy, R. K.; Clyburne, J. A. C. *Organometallics* **2007**, *26*, 6059–6062.
(43) Cooke, C. E.; Ramnial, T.; Jennings, M. C.; Pomeroy, R. K.; Clyburne, J. A. C. *Dalton Trans.* **2007**, 1755–1758.
(44) Ellul, C. E.; Saker, O.; Mahon, M. F.; Apperley, D. C.; Whittlesey, M. K. *Organometallics* **2008**, *27*, 100–108.
(45) Cabeza, J. A.; del Rio, I.; Miguel, D.; Sanchez-Vega, M. G. *Angew. Chem., Int. Ed.* **2008**, *47*, 1920–1922.
(46) Ellul, C. E.; Mahon, M. F.; Saker, O.; Whittlesey, M. K. *Angew. Chem., Int. Ed.* **2007**, *46*, 6343–6345.
(47) Cabeza, J. A.; del Rio, I.; Martinez-Mendez, L.; Miguel, D. *Chem. Eur. J.* **2006**, *12*, 1529–1538.
(48) Arnold, P. L. *Heteroat. Chem.* **2002**, *13*, 534–539.
(49) Ramnial, T.; Abernethy, C. D.; Spicer, M. D.; McKenzie, I. D.; Gay, I. D.; Clyburne, J. A. C. *Inorg. Chem.* **2003**, *42*, 1391–1393.
(50) De Fremont, P.; Scott, N. M.; Stevens, E. D.; Ramnial, T.; Lightbody, O. C.; Macdonald, C. L. B.; Clyburne, J. A. C.; Abernethy, C. D.; Nolan, S. P. *Organometallics* **2005**, *24*, 6301–6309.
(51) Lin, I. J. B.; Vasam, C. S. *Coord. Chem. Rev.* **2007**, *251*, 642–670.

Scheme 2. Reaction of $[Os_3(\mu\text{-}H)_2(CO)_{10}]$ with [(IMes)AgCl] Producing $[Os_3(\mu\text{-}H)(\mu\text{-}Cl)(CO)_9(IMes)]$ (1)

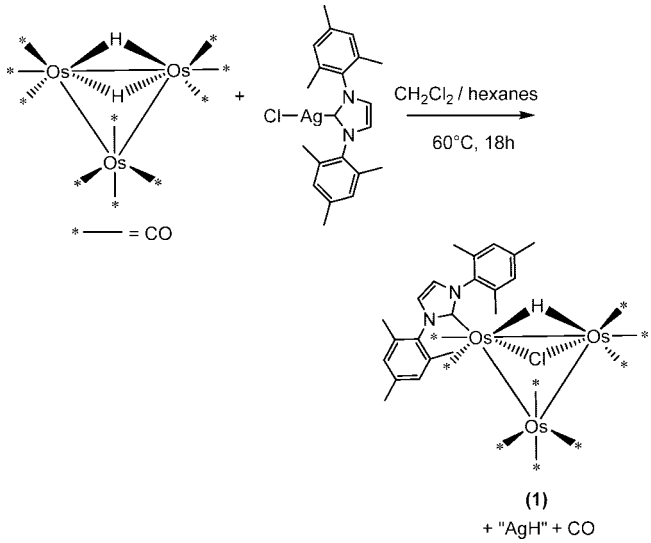

resonance integrated to a single hydrogen atom, which indicates that one of the hydrides had been lost from the osmium cluster.[54] Resonances are also present for the imidazolium ring protons and the 2,4,6-trimethylphenyl ring protons in the meta position.

In order to determine atom connectivity, X-ray crystallographic studies were performed on suitable single crystals of (**1**) grown from a concentrated solution in hexanes and toluene (Figure 3). The structure of (**1**) shows the anticipated formation of an NHC−osmium carbonyl cluster complex, but not the one predicted by Scheme 1. The molecule can be viewed as an NHC complex of the osmium carbonyl cluster $[Os_3(\mu\text{-}H)(\mu\text{-}Cl)(CO)_9]$, where an NHC occupies a coordination site previously engaged by a CO ligand in $[Os_3(\mu\text{-}H)_2(CO)_{10}]$, and a hydride ligand has been replaced by a chloride ligand. By mass balance, the reactants $[Os_3(\mu\text{-}H)_2(CO)_{10}]$ and [(IMes)AgCl] are incorporated into the final product with concomitant loss of AgH, which, presumably, disproportionates to elemental silver and H_2. LSIMS and elemental analysis of (**1**) gave results consistent with the proposed structure.

Selected bond lengths and angles associated with the solid state structure of (**1**), shown in Table 1, give a C(1)−Os bond

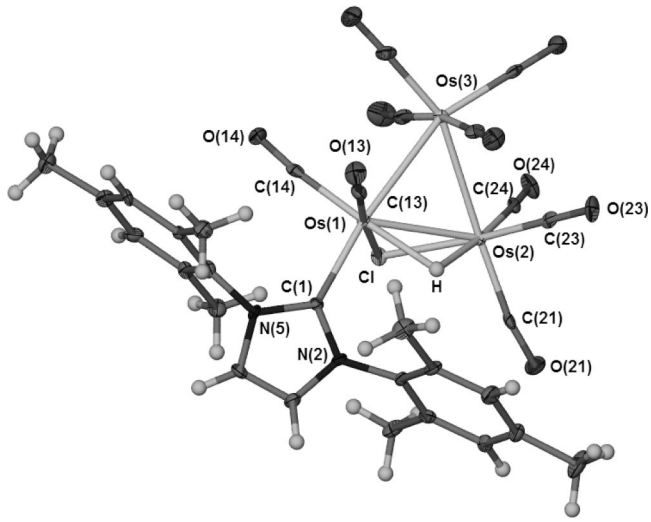

Figure 3. ORTEP view of $[Os_3(\mu\text{-}H)(\mu\text{-}Cl)(CO)_9(IMes)]$ (**1**). Ellipsoids are drawn at the 50% probability level.

Table 1. Selected Bond Lengths and Angles for $[Os_3(\mu\text{-}H)(\mu\text{-}Cl)(CO)_9(IMes)]$ (1)

Bond Lengths (Å)			
Os(1)−C(1)	2.121(6)	Os(2)-Cl	2.4566(16)
Os(1)−Os(2)	2.8536(4)	Os(1)-H	1.91(4)
Os(1)−Os(3)	2.8629(4)	Os(2)-H	1.91(4)
Os(2)−Os(3)	2.8414(3)	C(1)−N(5)	1.352(8)
Os(1)-Cl	2.4715(15)	C(1)−N(2)	1.371(7)

Bond Angles (°)			
C(1)−Os(1)−Os(3)	172.70(17)	N(5)−C(1)−Os(1)	126.6(4)
Os(2)−Os(1)−Os(3)	59.609(9)	O(13)−C(13)−Os(1)	178.9(6)
Os(3)−Os(2)−Os(1)	60.359(9)	O(14)−C(14)−Os(1)	173.6(6)
Os(2)−Os(3)−Os(1)	60.032(9)	O(21)−C(21)−Os(2)	169.9(6)
N(2)−C(1)−Os(1)	129.8(5)	O(22)−C(22)−Os(2)	175.3(6)
N(5)−C(1)−N(2)	103.4(5)	O(22)−C(22)−Os(2)	178.3(6)

distance of 2.121(6) Å, longer than the 2.056(7) Å for C(1)−Ag found in [(IMes)AgCl].[49]

Osmium−osmium bond lengths are all very close in value ranging from 2.8629(1) Å to 2.8414(3) Å. The metal−metal bond trans to the carbene is the longest in the complex, Os(1)−Os(3) 2.8629 Å, compared to 2.814(1) Å in the parent cluster.[53] While the bond cis to the carbene, Os(1)−Os(2) 2.8414(3) Å, is the shortest in the cluster, this bond also supports the bridging hydride and chloride atoms, lengthened from 2.683(1) Å in the parent cluster.[53] As the increase is notable, it may result from the much larger bridging chloride, which acts in concert with the strong donating abilities of the IMes ligand to lengthen all metal−metal bonds in the cluster. The steric influence of the bulky 2,4,6-trimethylphenyl substituent on neighboring carbonyls may also play a role in the lengthening of the metal−metal bonds to minimize steric crowding.[55]

Analysis of the bond angles of the carbonyls bonded to Os(1) and Os(2) reveal the effect of the bulky NHC ligand. The O(21)−C(21)−Os(2) angle is 169.9(6)°. It shows the largest deviation from linearity of all the carbonyls present in the cluster and is located closest to the NHC ligand. Surrounding M−C−O angles range from 173.6(6)° to 178.9(6)°. The longest carbonyl bond length is 1.158(8) Å, and the shortest is 1.127(8) Å for C(13)−O(13) and C(33)−O(33), respectively.

Interaction of the 2,4,6-trimethylphenyls group with carbonyls on the osmium to which the NHC is bonded and on the neighboring metal are most likely the reason why a separate transmetalation reaction of the free IMes could not be achieved on $[Os_3(CO)_{12}]$. Attempts were made on $[Os_3(CO)_{12}]$ when activated toward substitution chemically with trimethylamine *N*-oxide and also thermally by heating a solution of these reactants. All such reactions resulted in complete decomposition with no complexes isolable other than unreacted $[Os_3(CO)_{12}]$. These results mirror those recently found by Cabeza at al. for the reaction of free IMes wherein it is suggested that the carbene is too large to substitute a CO.[41]

A comparable NHC−osmium complex is the species $[Os_3(Me_2Im)(CO)_{11}]$ (Me_2Im = 1,3-dimethylimidazol-2-ylidene); a methyl-containing carbene derivative was found to have an osmium−carbene bond length of 2.116(9) Å and was prepared by Cabeza et al.[41] The NHC−triruthenium carbonyl complex of the formula $[Ru_3(Me_2Im)(CO)_{11}]$ was prepared by a similar method.[30] $[Os_3(Me_2Im)(CO)_{11}]$ and $[Ru_3(Me_2Im)(CO)_{11}]$ have

(52) Orpen, A. G. *J. Chem. Soc., Dalton Trans.* **1980**, 2509–2516.
(53) Orpen, A. G.; Rivera, A. V.; Bryan, E. G.; Pippard, D.; Sheldrick, G. M.; Rouse, K. D. *J. Chem. Soc., Chem. Commun.* **1978**, 723–724.
(54) Eady, C. R.; Johnson, B. F. G.; Lewis, J.; Malatesta, M. C. *J. Chem. Soc., Dalton Trans.* **1978**, 1358–1363.
(55) Biradha, K.; Hansen, V. M.; Leong, W. K.; Pomeroy, R. K.; Zaworotko, M. J. *J. Cluster Sci.* **2000**, *11*, 285–306.

the carbene attached in an equatorial position, and in (**1**), IMes is also attached in an equatorial position.[30,41]

$^{13}C\{^1H\}$ NMR solution studies on (**1**) are consistent with the asymmetry found in the ^1H NMR spectrum. $^{13}C\{^1H\}$ resonances at 18.6 ppm and 19.0 ppm of approximately equal intensity appear to be the *ortho*-methyl carbons. Analysis of the aromatic region of the $^{13}C\{^1H\}$ spectrum reveals two resonances for the arene carbon atoms at the C-3,5 and C-2,6 positions of the 2,4,6-trimethylphenyl rings of the IMes ligand, compared to a single resonance for both in Ar−C-3,5 and Ar−C-2,6 in [(IMes)AgCl].[49] Single resonances remain for the other carbon atoms, and it should be noted that the relative positions of the carbon resonances have shifted upfield by about 1 ppm. This can be attributed to the large electron rich center (osmium) to which IMes is now bound. From looking at the X-ray crystal structure ORTEP diagram, the asymmetry observed in the NMR spectra can be attributed to the proximity of the IMes ligand to the bridging chloride and hydride; the ortho-methyl groups closer to the chloride than to the hydride experience a different electronic environment.

In metal carbonyl clusters, the carbonyls generally undergo two types of fluxional processes: (1) rotation at the metal center and (2) exchange between metal centers via bridging intermediates. Therefore, if exchange was occurring among all atoms equally, a single peak would be observed since every carbonyl would appear equivalent. As temperature is decreased, the NMR spectrum will begin to exhibit a collapse and distinct peaks for each carbonyl can become evident.[56−58]

In the acquisition of the $^{13}C\{^1H\}$ NMR spectrum, the carbonyl region was well resolved. The region between 186 ppm to 169 ppm revealed nine resonances of approximate intensity 1 and a single resonance of intensity 0.5. As there are only nine carbonyls present in the cluster, it is believed that one of the resonances corresponds to the carbenic carbon, and it has been tentatively assigned to the signal at 176.3 ppm on the basis of its integration, as it is expected that the carbonyls would all have similar integrations due to similar relaxation rates. Furthermore, a carbene ^{13}C resonance at 169.8 ppm has been reported for the mononuclear complex [(η^6-p-cymene)$OsCl_2$-(IMes)][CF_3SO_3]; therefore, an assignment at 176.3 ppm is consistent with the handful of known mononuclear osmium−NHC complexes.[37,59] Conclusive assignment of each carbonyl resonance was not made; however, nine resonances confirm that the carbonyl groups are not fluxional at this temperature.

The preceding data suggest a new type of reactivity of NHC−silver(I) halides in organometallic cluster systems, involving the incorporation of not just the IMes carbene fragment but also the associated halide in hydrogen rich cluster species.

Characterization of [Os_3(μ-Cl)$(CO)_{10}$(μ-Ag(IMes)] (2). The reaction of the activated cluster [$Os_3(CO)_{10}(CH_3CN)_2$] with [(IMes)AgCl] is shown in Scheme 3. Displacement of acetonitrile ligands leads to the formation of [Os_3(μ-Cl)$(CO)_{10}$(μ-Ag(IMes))] (**2**) (49 mg, 35%) and the ionic compound [(IMes-H)][Os_3(μ-Cl)$(CO)_{10}$](μ_4-Ag)[Os_3(μ-Cl)$(CO)_{10}$] (**3**) (15 mg, 13%). The anticipated precipitation of $AgCl_{(s)}$ was not observed, and no solid material was formed during the reaction. The

Scheme 3. Reaction of [$Os_3(CO)_{10}(CH_3CN)_2$] with [(IMes)AgCl] Producing [Os_3(μ-Cl)$(CO)_{10}$(μ-Ag(IMes))] (2) and [(IMes-H)][Os_3(μ-Cl)$(CO)_{10}$](μ_4-Ag)[Os_3(μ-Cl)$(CO)_{10}$] (3)

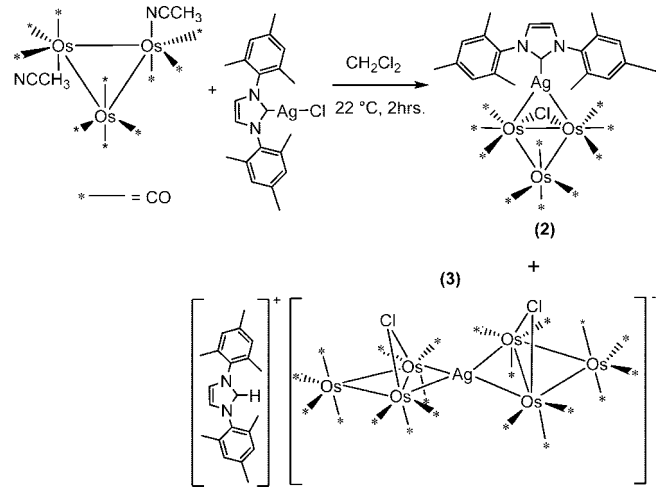

reaction of [(IMes)AgCl] with the activated osmium species, [$Os_3(CO)_{10}(CH_3CN)_2$], does not proceed via loss of AgCl, but rather a new type of reactivity is observed for NHC−silver(I) halide complexes.

^1H and ^{13}C NMR solution studies on the red crystalline solid material (**2**) revealed the presence of the IMes ligand with an *ortho*-methyl resonance at 1.83 ppm (12H) and a *para*-methyl resonance at 2.10 ppm (6H). A single resonance at 6.76 ppm was assigned to the *meta*-H of the 2,4,6-trimethylphenyl and a doublet at 6.89 ppm to the *imidazol*-H. IR solution studies on a hexanes solution indicated the presence of seven ν(CO) bands. Curiously, elemental analysis and LSIMS (M^+ *m*/*z* 1299.9) were consistent with the incorporation of ([(IMes)AgCl] into the cluster, with concomitant loss of acetonitrile.

In order to determine atom connectivity, we used crystallographic techniques. Single crystals of (**2**) were grown from hexanes and the results of the study are shown in Figure 4, with selected bond lengths and angles shown in Table 2.

As shown in Figure 4, the Ag−C bond is maintained in (**2**), but the Ag−Cl bond has been cleaved. Two new Ag−Os interactions were found, leading to an NHC−heterobimetallic complex.[11,51] The chloride atom was incorporated into a bridging position within the cluster such that the complex can be formulated as [Os_3(μ-Cl)$(CO)_{10}$(μ-Ag(IMes))]. Complex (**2**) is structurally related to [$Os_3(CO)_{10}$(μ-PPh_2)(μ-Ag$P(C_6H_5)_3$)], which was prepared in a multistep procedure, but the preparation of

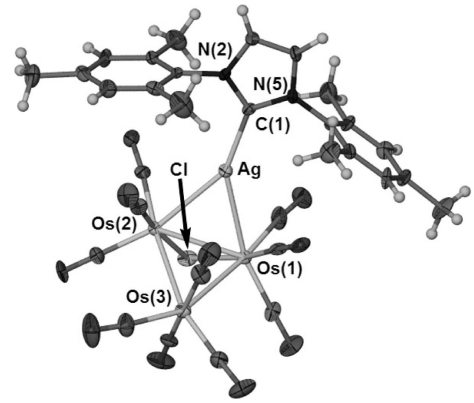

Figure 4. ORTEP view of [Os_3(μ-Cl)$(CO)_{10}$(μ-Ag(IMes))] (**2**). Ellipsoids are drawn at the 50% probability level.

(56) Crabtree, R. *The Organometallic Chemistry of the Transition Metals*, 4th ed.; John Wiley & Sons, Inc.: Hoboken, NJ, 2005.
(57) Dyson, P. J.; McIndoe, J. S. *Transition Metal Carbonyl Cluster Chemistry*; Gordon and Breach Science Publishers: Amsterdam, 2000.
(58) Johnson, B. F. G.; Benfield, R. E. *Transition Metal Clusters*; John Wiley & Sons: Chichester, England, 1980.
(59) Castarlenas, R.; Esteruelas, M. A.; Onate, E. *Organometallics* **2007**, *26*, 2129–2132.

Table 2. Selected Bond Lengths and Angles for $[Os_3(\mu\text{-Cl})(CO)_{10}(\mu\text{-Ag(IMes)}]$ (2)

Bond Lengths (Å)			
C(1)-Ag	2.120(12)	Os(1)−Os(2)	2.8179(8)
Os(2)-Ag	2.7983(11)	Os(1)−Os(3)	2.8435(8)
Os(1)-Ag	2.8071(13)	Cl−Os(1)	2.462(3)
C(1)−N(5)	1.348(15)	Cl−Os(2)	2.455(4)
C(1)−N(2)	1.334(16)		
Bond Angles (°)			
Os(2)−Cl-Os(1)	69.94(10)	Os(1)−Ag-Os(2)	60.36(3)
Os(2)−Ag-C(1)	150.5(4)	N(2)−C(1)−N(5)	104.9(11)
Os(1)−Ag-C(1)	148.8(4)	Os(2)−Os(3)−Os(1)	59.412(19)
Os(1)−Os(2)−Os(2)	60.305(19)	Os(2)−Os(1)−Os(3)	60.28(2)

this class of bimetallic butterfly complexes is best achieved using the synthetic methodology presented here.[60]

In order to determine if carbonyl groups were fluxional, ^{13}C NMR solution studies were performed on a sample of (**2**), which had been synthesized from $[Os_3(CO)_{10}(CH_3CN)_2]$ prepared with ^{13}C carbon monoxide and subjected to the reaction via the method described in the Experimental Section.[61] The appearance of six ^{13}C resonance signals indicates that at 25 °C the carbonyl ligands are not fluxional in solution.

To determine if any rearrangement or structural changes could occur, a sample of (**2**) was dissolved in hexanes and progressively heated. Analysis of the reaction solution by IR spectroscopy revealed bands in the ν(CO) region corresponding to the decomposition product $[Os_3(CO)_{12}]$ at temperatures greater than 90 °C. No further study was attempted.

Characterization of $[(IMes\text{-}H)][Os_3(\mu\text{-Cl})(CO)_{10}](\mu_4\text{-Ag})[Os_3(\mu\text{-Cl})(CO)_{10}]$ (3). The second compound isolated from the reaction of $[Os_3(CO)_{10}(CH_3CN)_2]$ with [(IMes)AgCl] was crystallized as a dark scarlet solid (Scheme 3). ^1H solution NMR on the scarlet crystalline solid material (**3**) revealed the presence of the $\{IMes\text{-}H\}^+$ ion with a distinct resonance signal at 8.25 ppm, which had not been present in (**2**). IR solution studies on a dichloromethane solution indicated the presence of six ν(CO) bands in a distinct pattern markedly different from the other IMes containing complexes.

Once again, X-ray crystallographic techniques were necessary to assign the atom connectivity in (**3**). Scarlet single crystals of (**3**) were grown, and the results of the study are shown in Figure 5. The results clearly show that the solid is composed of discrete $\{IMes\text{-}H\}^+$ ions and the new complex anion $\{[Os_3(\mu\text{-Cl})(CO)_{10}](\mu_4\text{-Ag})[Os_3(\mu\text{-Cl})(CO)_{10}]\}^-$. Associated bond lengths and angles are shown in Table 3.

The $\{[Os_3(\mu\text{-Cl})(CO)_{10}](\mu_4\text{-Ag})[Os_3(\mu\text{-Cl})(CO)_{10}]\}^-$ anion was confirmed by the observation of a major ion detected by

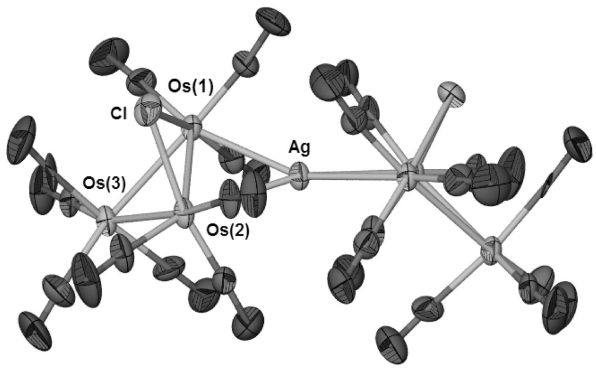

Figure 5. ORTEP view of the anionic component of $\{[Os_3(\mu\text{-Cl})(CO)_{10}](\mu_4\text{-Ag})[Os_3(\mu\text{-Cl})(CO)_{10}]\}^-$ (**3**). Ellipsoids are drawn at the 50% probability level.

Table 3. Selected Bond Lengths and Angles for $\{[Os_3(\mu\text{-Cl})(CO)_{10}](\mu_4\text{-Ag})[Os_3(\mu\text{-Cl})(CO)_{10}]\}^-$ (3)

Bond Lengths (Å)			
Os(2)-Cl	2.462(7)	Os(2)−Os(3)	2.8579(15)
Os(1)-Cl	2.455(6)	Os(1)−Os(3)	2.8583(14)
Ag−Os(2)	2.9015(10)	Os(2)−Os(1)	2.7805(14)
Ag−Os(1)	2.8597(12)		
Bond Angles (°)			
Os(1)−Cl-Os(2)	68.86(16)	Os(1)−Ag-Os(2)	57.71(3)
Os(2)−Os(1)−Os(3)	60.89(4)	Os(2)−Os(1)−Ag	61.90(3)
Os(1)−Os(2)−Os(3)	60.90(4)	Os(3)−Os(1)−Ag	109.17(6)
Os(2)−Os(3)−Os(1)	58.21(3)		

LSIMS studies (M^+ 1883.4 *m*/*z*), and elemental analysis on the bulk sample was in accord with this formulation.

Formation of the imidazolium species suggests the presence of water in the reaction vessel, despite flame drying of the apparatus and the use of a dry nitrogen atmosphere. Repeated experiments to generate compounds (**2**) and (**3**) under rigorously dry conditions resulted in similar isolated yields, thus suggesting that abstraction of H^+ may come from another source, such as CH_2Cl_2, which was previously distilled and stored over calcium hydride.

The structure of (**3**) is similar to that reported for $[(Ph_3P)_2N]^+[\{Os_3H(CO)_{10}\}_2Ag]^-$ by Raithby et al.[62] The structure of (**3**) can be considered as saturated as it contains 48 skeletal electrons required if metal−metal bonds are considered to be composed of localized two-center two-electron interactions between osmium atoms.[62] The Os(1)−Os(2) bond is doubly bridged by a one-electron donor (Ag) and a three-electron donor (Cl).[62] The bridged Os−Os bonds found in (**3**) are shorter by about 0.08 Å than the unbridged bonds, which is not short enough to be consistent with double bond character, typically about 0.15 Å shorter.[63]

The formation of (**3**) is believed to be the result of an equilibrium occurring in the [(IMes)AgCl] species (Scheme 4).[11] The labile nature of the silver−carbene bond influences the formation silver−silver contacts and molecular aggregation to generate novel structural motifs.[11] The $[AgCl_2]^-$ ion is believed to react with two molecules of $[Os_3(CO)_{10}(CH_3CN)_2]$, following acetonitrile loss such that it leads to its complete incorporation into (**3**).

To further confirm the structure, a ^{13}C CO-enriched sample of (**3**) was prepared and subjected to $^{13}C\{^1H\}$ NMR solution studies. Results of this study revealed the presence of six distinct resonances in the carbonyl region. The ^{13}C NMR spectrum contains resonances expected for a complex exhibiting the symmetry and carbonyls associated with (**3**).

To determine if any thermal rearrangement could occur, a small amount of (**3**) was heated at progressively higher temperatures in CH_2Cl_2 up to 110 °C. Analysis of the reaction mixture by IR spectroscopy revealed bands in the ν(CO) region consistent with $[Os_3(CO)_{12}]$, suggesting the complex decomposed under heating. A dark solid which was not soluble in CH_2Cl_2 was also present. No other novel reaction products could be isolated; further study was not attempted.

Trinuclear-osmium cluster compounds have given unpredictable reaction products when treated with [(IMes)AgCl], an NHC

(60) Ahrens, B.; Cole, J. M.; Hickey, J. P.; Martin, J. N.; Mays, M. J.; Raithby, P. R.; Teat, S. J.; Woods, A. D. *Dalton Trans.* **2003**, 1389–1395.
(61) Alex, R. F.; Pomeroy, R. K. *Organometallics* **1987**, *6*, 2437–2446.
(62) Fajardo, M.; Gomez-Sal, M. P.; Holden, H. D.; Johnson, B. F. G.; Lewis, J.; McQueen, R. C. S.; Raithby, P. R. *J. Organomet. Chem.* **1984**, *267*, C25−C28.
(63) Churchill, M. R.; Hollander, F. J.; Hutchinson, J. P. *Inorg. Chem.* **1977**, *16*, 2697–2700.

Scheme 4. Equilibrium in NHC Ag(I) Chloride Species Leading to the Formation of Ion Pairs

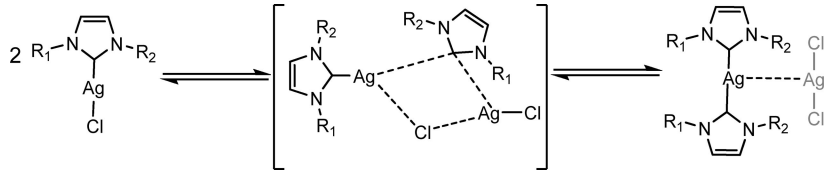

transfer reagent.[43] As osmium carbonyl compounds can be synthesized containing a higher number of metal atoms, it was desirable to study their reactions with [(IMes)AgCl].[57,58,64−66]

2. Successful NHC Transfer Chemistry. Upon examination of our previous results, it was found that $[Os_3(\mu\text{-}H)_2(CO)_{10}]$ using [(IMes)AgCl] undergoes transmetalation, replacing a carbonyl ligand with IMes. However, the reaction also resulted in the replacement of a bridging hydride with a bridging chloride. In considering what led to this result, we suggest that the more open (less sterically hindered) metal framework that resulted from replacing carbonyl groups with hydrides plays a large role in successful transmetalation. Furthermore, to facilitate NHC transfer we again introduced a leaving group onto the cluster and used mild reaction conditions.

Characterization of $[Os_4(\mu\text{-}H)_4(CO)_{11}(n\cdot IMes)]$ (4). $[Os_4(\mu\text{-}H)_4(CO)_{12}]$ was activated toward substitution by the use of trimethylamine *N*-oxide, a convenient decarbonylation reagent.[67] Reaction of the activated complex with 1,3-bis-(2,4,6-trimethylphenyl)imidazol-2-ylidene-silver(I) chloride [(IMes)AgCl] produced a crystalline solid characterized (vide infra) as $[Os_4(\mu\text{-}H)_4(CO)_{11}(n\cdot IMes)]$ (**4**). This is believed to be the first example of an NHC transfer agent displaying typical transfer reactivity toward cluster compound, as previously communicated.[42] The reaction of $[Os_4(\mu\text{-}H)_4(CO)_{12}]$ with [(IMes)AgCl] in dichloromethane at room temperature was accomplished by the removal of a carbonyl with trimethylamine *N*-oxide (Scheme 5). $AgCl_{(s)}$ was seen to precipitate as a gray−white solid.

Scheme 5. Reaction of $[Os_4(\mu\text{-}H)_4(CO)_{12}]$ with [(IMes)AgCl] Using $(CH_3)_3NO$ as a Decarbonylation Agent, Producing $[Os_4(\mu\text{-}H)_4(CO)_{11}(n\cdot IMes)]$ (4)

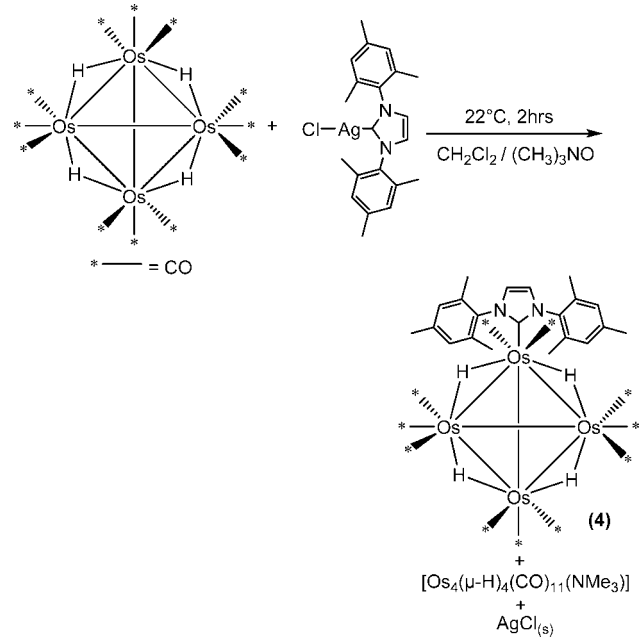

^1H solution NMR studies of (**4**) in CD_2Cl_2 revealed the presence of the IMes ligand in addition to four bridging hydride ligands, which were found to be fluxional (−20.1 ppm, broad). ^{13}C solution NMR studies confirmed the presence of the IMes ligand, displaying resonances for the imidazole ring and the 2,4,6-trimethylphenyl carbons. IR studies of a CH_2Cl_2 solution exhibit nine ν(CO) bands. The composition of (**4**) was supported by elemental analysis and LSIMS ($M^+ = m/z$ 1377.9).

To determine the atom connectivity, we used X-ray crystallographic techniques. Single yellow crystals of (**4**) were grown in a mixture of CH_2Cl_2 and hexanes; the ORTEP view is shown in Figure 6. The study determined that there were two crystallographically unique but structurally similar molecules in the unit cell. Table 4 contains selected bond lengths and angles. The structure of (**4**) contains an IMes ligand bound to an osmium cluster, with a single carbon−osmium bond, C(1)−Os(1), which is 2.05(3) Å long. The other molecule in the asymmetric unit has a C(6)−Os(5) bond length of 2.20(3) Å. In the cluster, osmium−osmium bond distances are consistent with those of clusters containing bridging hydrides; therefore, the hydrides are placed on the long bonds within the osmium core.[68,69] Osmium−osmium bonds supporting bridging hydrides were found to have lengths ranging from 2.990(2) Å to 2.938(2) Å. Osmium−osmium distances without hydride ligands were found to range from 2.826(3) Å to 2.8091(11) Å, clearly differentiating them from hydride-supporting bonds. Usually, the positions of the hydride ligands can be inferred reliably from the positions of the longer metal−metal edges; the result here further confirms the usefulness of such correlations.[65,69,70] Osmium-hydride positions were inserted into the crystal data and refined with final values found to be 1.67(4) Å.

The M_4H_4 family of clusters is known to exist in two predominant geometries: a D_{2d} form and a C_s form (Figure

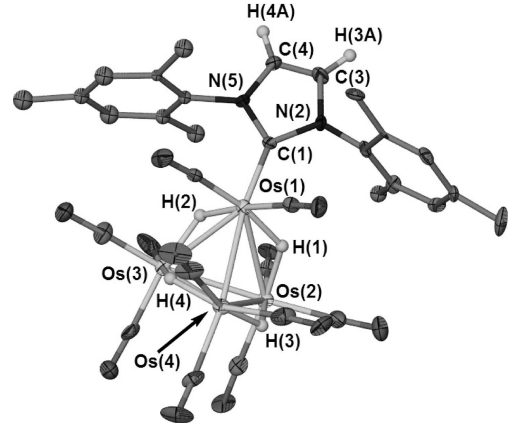

Figure 6. ORTEP view of $[Os_4(\mu\text{-}H)_4(CO)_{11}(n\cdot IMes)]$ (**4**). Ellipsoids are drawn at the 50% probability level. 2,4,6-Trimethylphenyl hydrogens have been omitted for clarity.

(64) Cotton, F. A.; Wilkinson, G.; Murillo, C. A. *Advanced Inorganic Chemistry*, 6th ed.; Wiley: New York, 1999.
(65) Pomeroy, R. K. *Comphrehensive Organometallic Chemistry II*, 2nd ed.; Elsevier Science Ltd.: Terrytown, NY, 1995; Vol. 7.
(66) Shriver, D. F.; Atkins, P. W.; Langford, C. H. *Inorganic Chemistry*; W. H. Freeman and Company: New York, 1990.
(67) Luh, T. Y. *Coord. Chem. Rev.* **1984**, *60*, 255–276.

Table 4. Selected Bond Lengths and Angles for $[Os_4(\mu\text{-}H)_4(CO)_{11}(n\cdot IMes)]$ (4)

Bond Lengths (Å)			
Os(1)−Os(4)	2.826(3)	Os(3)−Os(4)	2.9778(13)
Os(1)−Os(3)	2.938(2)	Os(1)−C(1)	2.05(3)
Os(1)−Os(2)	2.988(2)	C(43)−O(43)	0.98(3)
Os(2)−Os(3)	2.8091(11)	C(1)−N(2)	1.43(3)
Os(2)−Os(4)	2.9524(11)	C(1)−N(5)	1.44(3)
Bond Angles (°)			
C(1)−Os(1)−Os(3)	117.0(8)	N(2)−C(1)−Os(1)	131.2(16)
C(1)−Os(1)−Os(2)	108.9(11)	Os(4)−Os(1)−Os(3)	62.18(6)
C(1)−Os(1)−Os(4)	169.1(9)	Os(4)−Os(1)−Os(2)	60.96(5)
N(5)−C(1)−N(2)	97(3)	Os(3)−Os(1)−Os(2)	56.58(5)
N(5)−C(1)−Os(1)	131.9(17)		

Table 5. Selected Bond Lengths and Angles for $[Os_4(\mu\text{-}H)_4(CO)_{10}(IMes)_2]$ (5)

Bond Lengths (Å)			
Os(1)−C(11)	2.119(10)	Os(2)−Os(4)	2.8293(6)
Os(2)−C(21)	2.120(11)	Os(2)−Os(3)	2.9429(6)
Os(1)−Os(4)	3.0074(7)	Os(3)−Os(4)	2.8014(7)
Os(1)−Os(3)	3.0361(6)	C(4)−O(4)	1.118(14)
Os(1)−Os(2)	3.0532(6)	C(7)−O(7)	1.106(15)
C(11)−N(15)	1.356(14)	C(21)−N(25)	1.342(14)
C(11)−N(12)	1.382(14)	C(21)−N(22)	1.366(15)
C(13)−C(14)	1.319(19)	C(23)−C(24)	1.32(2)
C(14)−N(15)	1.355(15)	C(23)−N(22)	1.340(16)
C(13)−N(12)	1.426(15)	C(24)−N(25)	1.394(16)
Bond Angles (°)			
Os(4)−Os(1)−Os(3)	55.228(15)	Os(4)−Os(3)−Os(2)	58.955(16)
Os(4)−Os(1)−Os(2)	55.228(15)	Os(4)−Os(3)−Os(1)	61.865(16)
Os(3)−Os(1)−Os(2)	57.801(14)	Os(2)−Os(3)−Os(1)	61.390(15)
Os(4)−Os(2)−Os(3)	58.026(16)	Os(3)−Os(4)−Os(2)	63.019(16)
Os(4)−Os(2)−Os(1)	61.353(15)	Os(3)−Os(4)−Os(1)	62.906(16)
Os(3)−Os(2)−Os(1)	60.809(15)	Os(2)−Os(4)−Os(2)	62.993(15)
N(15)−C(11)−N(12)	104.5(9)	N(25)−C(21)−N(22)	103.0(10)
N(15)−C(11)−Os(1)	129.3(8)	N(25)−C(21)−Os(2)	128.2(9)
N(12)−C(11)−Os(1)	126.1(8)	N(25)−C(21)−Os(2)	128.4(9)

14).[70,71] Of these two, the D_{2d} form is more common. The energy difference between the geometries is small, a conclusion that is supported by the observation that the hydride atoms are fluxional on the NMR time scale at ambient temperature.[70] The Os_4H_4 core of molecule (**4**) has pseudo D_{2d} symmetry, with four long and two short metal−metal distances commonly found in the $[Os_4H_4(CO)_{12}]$/$[Ru_4H_4(CO)_{12}]$ family of compounds.[70]

Given the symmetry of the solid-state structure of (**4**), it would be expected that if the hydrides were nonfluxional, the resulting pattern in the hydride region of the ^{1}H NMR spectrum would be a 2:2 ratio of peaks, as a mirror plane bisecting the molecule would make for two pairs of equivalent hydrides. Given that the barrier to hydride motion is small, the result is a broad single resonance at room temperature.[71] Low-temperature NMR solution studies were used to determine if the solid state structure was the same as the rigid solution structure, at temperatures ranging from 22 to −90 °C. A figure of this study is provided in Supporting Information.

At $T = 0$ to −20 °C, the hydride motion begins to slow such that multiple resonances of individual hydrides are evident. The spectrum at −20 °C reveals resonances that appear consistent with both conformers. Upon further cooling (T= −30 to −40 °C), the broad resonances at 20.6 ppm and 20.8 ppm begin to collapse. Concurrently, three resonances at −19.8 ppm, −20.2 ppm, and −21.3 ppm sharpen. The spectrum at −70 °C contains three peaks believed to correspond to a C_s conformer in the 1:2:1 pattern. Although it is expected that a C_s type arrangement of hydrides would result in a 1:1:1:1 pattern, it appears either that there is no significant chemical shift difference or that some measure of hydride motion is still active. The resonances in the spectra at −80 and −90 °C begin to broaden because of the insolubility of the compound.

Variable temperature studies were performed on a sample of (**4**) labeled with ^{13}CO gas. $^{13}C\{^1H\}$ NMR solution studies were performed at 22 and 5 °C. At 22 °C, two sharp resonances are observed: one at 177.3 ppm integrating to three carbon atoms and one at 166.6 ppm integrating to two carbon atoms. A third slightly broadened resonance is observed at 171.8 ppm between two weak signals, which appear to be collapsing into the baseline. This signal integrated to four carbon atoms. Of the collapsing signals seen, the broad signal at 174.6 ppm was the stronger of the two. At 5 °C, the carbonyl exchange appears to be slowing, as the central resonance at 171.6 ppm begins to become asymmetric and collapse into the baseline. This is accompanied by the growth of two previously weak resonances at 175.6 ppm and 169.3 ppm. Further cooling would result in these two resonances becoming sharp, and all fluxional motion would cease. We conclude that the cessation of fluxional carbonyl motion is parallel to that of the hydrides.

The IMes ligand is oriented cis to two Os−H−Os edges and trans to an Os−Os bond. Similar orientations are found in $[Os_4H_4(CO)_{11}P(OMe)_3]$ and its ruthenium analogue.[70]

The results here suggest that successful transfer of the NHC fragment is dependent upon the steric constraints and the metal site to which the carbene is intended to be transferred. Careful choice of the reacting cluster is needed to ensure efficient transfer.

Characterization of $[Os_4(\mu\text{-}H)_4(CO)_{10}(IMes)_2]$ (5). Two NHCs can be added to $[Os_4(\mu\text{-}H)_4(CO)_{12}]$ using the displacement of two acetonitrile ligands from $[Os_4(\mu\text{-}H)_4(CO)_{10}(CH_3CN)_2]$. This complex is formed by the reaction of $[Os_4(\mu\text{-}H)_4(CO)_{12}]$ with trimethylamine *N*-oxide in a solution of CH_3CN. Addition of two equivalents of [(IMes)AgCl] results in the formation of $[Os_4(\mu\text{-}H)_4(CO)_{10}(IMes)_2]$ (**5**) (74 mg, 45%) (Scheme 6).

$[Os_4(\mu\text{-}H)_4(CO)_{10}(CH_3CN)_2]$ was generated *in situ* because of its reactive nature and its presence confirmed by identification with IR solution studies. The data is consistent with that previously reported.[72] Heating at 60 °C was found to be necessary to overcome the energy barrier to adding a second bulky ligand. Attempts to perform this reaction under ambient conditions were met with excessive decomposition.

A word about the isolation of (**5**) is in order: After the reaction to form $[Os_4(\mu\text{-}H)_4(CO)_{10}(CH_3CN)_2]$ with [(IMes)AgCl], the solvent is removed, and the residue is redisssolved in dichloromethane. After placement on the column, an orange band of (**5**) can be rapidly eluted. If care is not taken, this orange band will decompose on the column to produce a green material that can be further separated on the same column. After column chromatography on the recovered solid, LSIMS analysis (M^+ m/z 1654.0) suggested a tetranuclear cluster containing two IMes ligands. IR studies of CH_2Cl_2 solution of (**5**) indicated the presence of seven ν(CO) bands. Analysis of the orange crystals of (**5**) in solution by ^{1}H NMR spectroscopy solution studies revealed the presence of two IMes ligands and four bridging hydride ligands. Six ^{1}H resonances in the methyl region

(68) Churchill, M. R.; Hollander, F. J. *Inorg. Chem.* **1980**, *19*, 306–310.
(69) Churchill, M. R. *Adv. Chem. Ser.* **1978**, *167*, 36–60.
(70) Wei, C.-Y.; Garlaschelli, L.; Bau, R. *J. Organomet. Chem.* **1981**, *213*, 63–78.
(71) Pomeroy, R. K.; Leong, B. K. In Comprehensive Organometalic Chemistry, III; Crabtree, R. H., Mingos, D. M. P., Eds.; Elsevier Ltd.: New York, 2007; Vol. 6, pp 873−1044.
(72) Johnson, B. F. G.; Blake, A. J.; Martin, C. M.; Braga, D.; Parisini, E.; Chen, H. *J. Chem. Soc., Dalton Trans.* **1994**, 2167–2175.

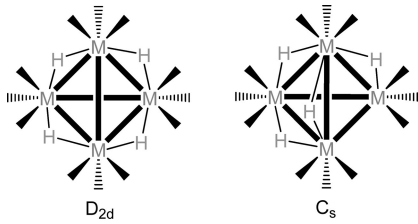

Figure 7. Two predominant geometries for the M_4H_4 family of clusters.

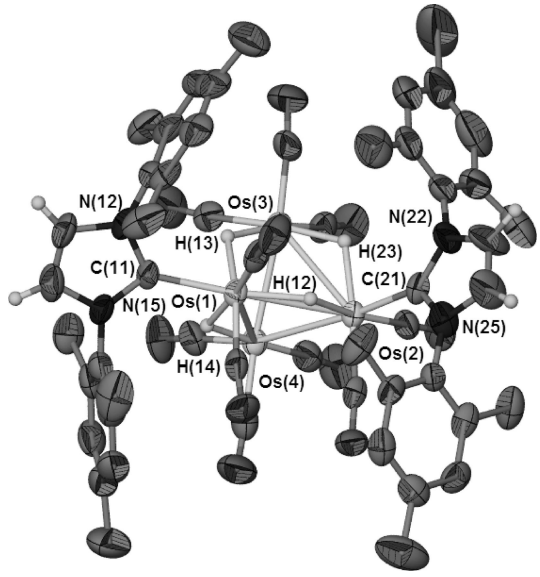

Figure 8. ORTEP view of $[Os_4(\mu\text{-}H)_4(CO)_{10}(IMes)_2]$ (**5**). Ellipsoids are drawn at the 50% probability level. 2,4,6-Trimethylphenyl hydrogens have been omitted for clarity.

integrating to 6 hydrogen atoms each as well as four individual hydride signals suggested a lowering of symmetry. The aromatic region displayed four broad singlets for the 2,4,6-trimethylphenyl ring hydrogens and two sharp resonances assigned to the imidazole ring hydrogens. All peaks in this region integrated to two hydrogen atoms, again consistent with two NHC ligands present.

$^{13}C\{^1H\}$ solution NMR studies confirmed the presence of the IMes ligands in a low-symmetry orientation. Aromatic carbon resonances are no longer equivalent for the 2,4,6-trimethylphenyl ring carbons and display a pattern that is consistent with rotation about the carbon−nitrogen bond and the osmium−carbon (carbene) bond. Observation and assignment of the two carbene singlets would be difficult as they are expected to fall in the same region as the carbonyls.[40,59]

X-ray crystallographic techniques were used to confirm the presence of the two NHC ligands and, in particular, to determine their relative placement in the cluster. The results of the X-ray study are shown in Figure 8 and in Table 6.

The hydride ligands of (**5**) were not located in the Fourier maps, but their positions have been assigned as bridging the long metal−metal bonds previously noted through use of Orpen's XHYDEX program (see Experimental Section for details).[53] XHYDEX predicted that the placement of the H ligands across the bonds Os(1)−Os(2), Os(1)−Os(3), Os(1)−Os(4), and Os(2)−Os(3) leads to a C_s type arrangement, which differs from that found in (**4**).

The presence of a second NHC ligand has caused the hydride ligands to be stationary, as four sharp resonances are observed

Table 6. Selected Bond Lengths and Angles for $[Os_4(\mu\text{-}H)_3(\mu\text{-}Cl)(CO)_{11}(IMes)]$ (6)

Bond Lengths (Å)			
Os(1)−C(1)	2.11(3)	Os(1)−H(12)	1.990(10)
Os(1)−Os(3)	2.9714(14)	Os(1)−H(13)	2.08(9)
Os(1)−Os(4)	3.0463(17)	Os(1)−H(14)	1.990(11)
Os(1)−Os(2)	3.0622(17)	Os(2)−H(12)	1.989(10)
Os(2)−Os(3)	2.8518(17)	Os(3)−H(13)	2.09(9)
Os(3)−Os(4)	2.8319(16)	Os(4)−H(14)	1.990(10)
C(1)−N(2)	1.35(4)	Os(2)−Cl(1)	2.474(7)
C(1)−N(5)	1.41(4)	Os(4)−Cl(1)	2.454(8)
N(2)−C(3)	1.37(4)	Os(2)−Os(4)	3.631
Bond Angles (°)			
C(1)−Os(1)−Os(3)	161.9(8)	Os(4)−Os(3)−Os(2)	79.41(4)
C(1)−Os(1)−Os(4)	117.7(8)	Os(4)−Os(3)−Os(1)	63.27(4)
Os(3)−Os(1)−Os(4)	56.13(4)	Os(2)−Os(3)−Os(1)	63.41(4)
C(1)−Os(1)−Os(2)	106.1(7)	N(2)−C(1)−N(5)	103(2)
Os(3)−Os(1)−Os(2)	56.39(4)	N(2)−C(1)−Os(1)	130(2)
Os(4)−Os(1)−Os(2)	72.94(4)	N(5)−C(1)−Os(1)	125.0(19)
Os(3)−Os(2)−Os(1)	60.20(4)		

in the ^1H NMR.[73] The osmium hydride distances were found to be 1.75(3) Å for Os(1)−H(13) and Os(3)−H(13), and the remaining were found to be 1.76(3) Å, longer than in (**4**).

The longest metal−metal bonds in (**5**) are those with bridging hydrides, the range being 3.0532(6) Å, for Os(1)−Os(2), to 2.9429(6) Å. Bonds without hydrides were shorter at 2.8293(6) Å and 2.8014(7) Å. This is not surprising given the steric interaction between adjacent NHC ligands, interactions which would be minimized by a lengthening of the metal−metal bond. Also, hydride supporting bonds are known to be longer in osmium clusters. Additionally, the increased electron density on the osmium atoms provides for better orbital overlaps in the metal−metal bonds.

The $^{13}C\{^1H\}$ and ^{13}C NMR spectra of (**5**) were acquired from a ^{13}CO enriched sample to study the carbonyl region at 25 °C. The presence of weak signals from 175.2 ppm to 183.5 indicates fluxional behavior on the NMR time scale. Integration of the region suggests six carbon atoms, although this is likely unreliable. Sharp resonances at 164.3 ppm, 171.2 ppm, and 173.0 ppm integrate in a 1:1:2 ratio. These resonances show coupling to the hydrides and are likely due to the carbonyl ligands on the osmium atoms to which IMes is bound. Similar to phosphines derivatives, these carbonyls would likely be restricted in motion about those metal centers.[74,75] Assignment of individual carbonyls was not attempted.

Synthesis of $[Os_4(\mu\text{-}H)_3(\mu\text{-}Cl)(CO)_{11}(IMes)]$ (6). When $[Os_4(\mu\text{-}H)_4(CO)_{10}(IMes)_2]$ (**5**) was subjected to column chromatography on 200-mesh silica gel 60, the bright orange complex changed color to dark green when left on the column for more than 10 min. The collected fractions changed color back to orange overnight. To determine what products resulted from this redistribution and hence to understand what process was at work, the compounds present in the time-lapsed orange solution were isolated (Scheme 7).

The discovery of $[Os_4(\mu\text{-}H)_4(CO)_{12}]$, the parent carbonyl for the tetranuclear reactions, was perhaps expected as several substitution reactions involving CH_3CN ligands with $[Os_3(CO)_{12\text{-}X}(CH_3CN)_X]$ (X = 1, 2) result in the formation of the parent carbonyl $[Os_3(CO)_{12}]$.[61,76] The isolated $[Os_4(\mu\text{-}H)_4(CO)_{11}(IMes)]$

(73) Band, E.; Muetterties, E. L. *Chem. Rev.* **1978**, *78*, 639–658.
(74) Mann, B. E.; Taylor, B. F. *^{13}C NMR Data for Orgnanometallic Compounds*; Academic Press: New York, 1981.
(75) Martin, L. R.; Einstein, F. W. B.; Pomeroy, R. K. *Organometallics* **1988**, *7*, 294–304.
(76) Martin, L. R.; Einstein, F. W. B.; Pomeroy, R. K. *J. Am. Chem. Soc.* **1986**, *108*, 338–340.

Scheme 6. Reaction of $[Os_4(\mu\text{-}H)_4(CO)_{10}(CH_3CN)_2]$ with [(IMes)AgCl] to Yield $[Os_4(\mu\text{-}H)_4(CO)_{10}(IMes)_2]$ (5) and the Complex Green Reaction Mixture

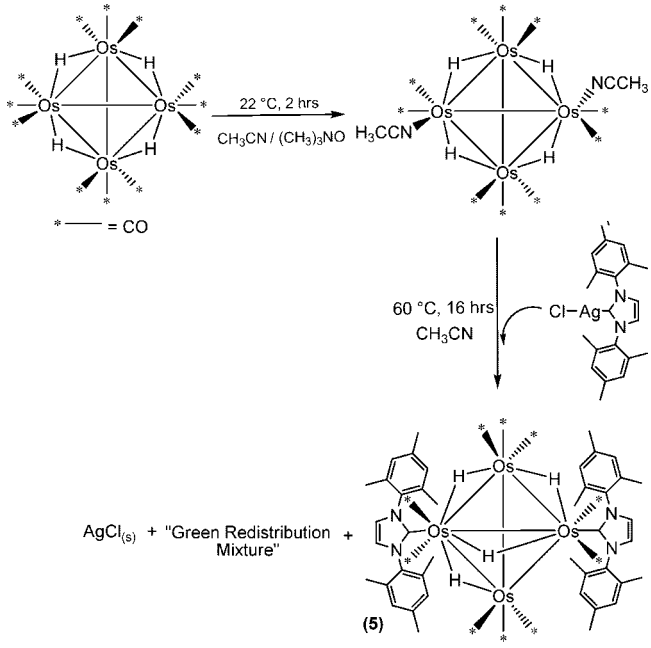

Scheme 7. Complexes Isolated by Column Chromatography of the Green Mixture: Isolation of $[Os_4(\mu\text{-}H)_3(\mu\text{-}Cl)(CO)_{11}(IMes)]$ (6)

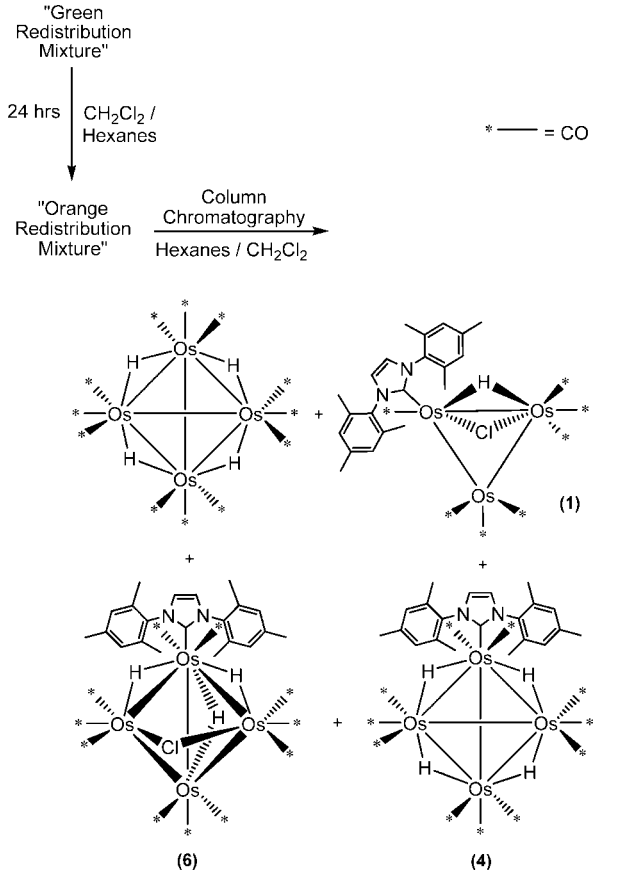

(**4**) was probably formed from trace quantities of $[Os_4(\mu\text{-}H)_4(CO)_{11}(CH_3CN)]$. However, the isolation of $[Os_3(\mu\text{-}H)(\mu\text{-}Cl)(CO)_9(IMes)]$ (**1**) was completely unexpected since no trinuclear starting material was present. The presence of (**1**) was confirmed by NMR and IR spectroscopy. The fourth compound,

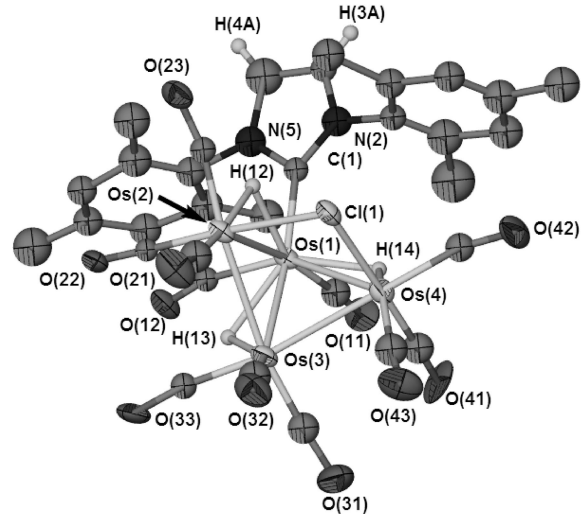

Figure 9. ORTEP view of $[Os_4(\mu\text{-}H)_3(\mu\text{-}Cl)(CO)_{11}(IMes)]$ (**6**). Ellipsoids are drawn at the 50% probability level.

a yellow solid, was determined to be $[Os_4(\mu\text{-}H)_3(\mu\text{-}Cl)(CO)_{11}(IMes)]$ (**6**). IR studies on a CH_2Cl_2 solution of (**6**) indicated the presence of seven ν(CO) bands.

^{1}H NMR studies revealed the presence of an IMes ligand as well as two hydride resonances in a 2:1 intensity ratio, leading to the conclusion that three hydrides were present. The $^{13}C\{^1H\}$ NMR spectrum displayed resonances consistent with that of the IMes ligand, with the carbene carbon resonance tentatively assigned at 150.7 ppm. X-ray crystallography revealed the atom connectivity shown in Figure 9; selected bond lengths and angles are presented in Table 7. LSIMS analysis agreed with the formulated structure.

The X-ray diffraction data were weak and not well resolved, with the structure being refined as an inversion twin and the crystal suspected to have desolvated. Thus, the solution to the X-ray data, albeit not stellar, confirms the connectivity. While the starting material contained a tetrahedral metal skeleton, (**6**) has a butterfly (nonplanar) arrangement. The X-ray structure reveals a tetranuclear osmium cluster in which one of the metal−metal bonds of (**5**) appears to have been broken, supplanted by a bridging chloride. Two chemically identical but crystallographically unique molecules are found in the unit cell. They differ in the orientation of the 2,4,6-trimethylphenyl groups, likely an effect of crystal packing.

This 62-electron *arachno* structure is unusual in that the precursor (**5**) and the combination of the IMes ligands and the hydride ligands appear to have been responsible for breaking the metal−metal bond. The presence of the trinuclear species (**1**) in the reaction mixture suggests a systematic breaking of bonds possibly promoted by the silica in the column in the presence of dichloromethane. It is suggested that the presence of two IMes ligands creates a crowded environment in which the Os(1)−Os(2) of (**5**) is weakened by steric interactions between the IMes fragments. This has recently been observed for triruthenium carbonyl clusters, which have been reacted with an excess of NHC such that they result exclusively in the formation of mononuclear ruthenium bis-NHC complexes.[44]

The source of the chloride, which replaced one of the hydrides in (**5**), is speculated to be abstracted either from AgCl or more likely from dichloromethane in the presence of silica, possibly due to the acidity of the column material. Hydride species are known to be susceptible to attack by chlorinated solvents; this

Table 7. Selected Bond Lengths and Angles for $[Os_5(\mu_5\text{-}C)(\mu\text{-}H)(CO)_{14}(\eta\text{-}C\text{-}\eta\text{-}N\text{-}C_2H_2(Mes)]$ (8)

Bond Length (Å)			
Os(1)−Os(2)	2.8691(5)	Os(1)−C(100)	2.073(9)
Os(1)−Os(3)	2.8617(5)	Os(2)−C(100)	1.989(9)
Os(1)−Os(5)	2.9300(5)	Os(3)−C(100)	1.994(9)
Os(2)−Os(4)	2.9286(6)	Os(4)−C(100)	2.093(9)
Os(2)−Os(5)	2.8734(5)	Os(5)−C(100)	2.126(8)
Os(3)−Os(4)	2.9172(5)	N(2)−C(1)	1.375(10)
Os(3)−Os(5)	2.8802(5)	N(2)−C(3)	1.371(11)
Os(4)−N(5)	2.112(7)	N(5)−C(1)	1.375(11)
Os(1)−C(1)	2.057(8)	N(5)−C(4)	1.393(11)
C(3)−C(4)	1.348(13)	O(42)−C(42)	1.123(11)
C(3)−H(31)	0.931	O(52)−C(52)	1.150(11)
C(4)−H(41)	0.937	Os(1)−H(3)	2.340
Os(1)−Os(4)	3.673	Os(5)−H(3)	2.210

Bond Angle (°)			
Os(2)−Os(1)−Os(3)	88.009(16)	Os(2)−Os(1)−C(1)	89.0(2)
Os(2)−Os(1)−Os(5)	59.392(13)	Os(3)−Os(1)−C(1)	87.5(2)
Os(3)−Os(1)−Os(5)	59.630(13)	Os(5)−Os(1)−C(1)	132.7(2)
Os(1)−Os(2)−Os(4)	78.604(14)	C(1)−Os(1)−C(10)	97.4(4)
Os(1)−Os(2)−Os(5)	61.360(13)	C(1)−Os(1)−C(11)	97.3(4)
Os(4)−Os(2)−Os(5)	88.628(17)	C(1)−Os(1)−C(100)	86.2(3)
Os(1)−Os(3)−Os(4)	78.912(14)	Os(1)−Os(2)−C(100)	46.3(2)
Os(1)−Os(3)−Os(5)	61.366(13)	Os(4)−Os(2)−C(100)	45.6(2)
Os(4)−Os(3)−Os(5)	88.719(14)	Os(5)−Os(2)−C(100)	47.7(2)
Os(3)−Os(4)−Os(2)	85.851(16)	C(21)−Os(2)−C(100)	116.2(4)
Os(1)−Os(5)−Os(3)	59.005(13)	C(22)−Os(2)−C(100)	128.9(4)
Os(1)−Os(5)−Os(2)	59.248(13)	C(23)−Os(2)−C(100)	119.1(4)
Os(3)−Os(5)−Os(2)	87.570(14)	Os(5)−C(100)−Os(4)	147.8(4)
N(5)−Os(4)−C(43)	176.4(4)	Os(5)−C(100)−Os(1)	88.5(3)
Os(4)−N(5)−C(1)	125.2(6)	Os(4)−C(100)−Os(1)	123.7(4)
Os(4)−N(5)−C(4)	125.7(6)	Os(5)−C(100)−Os(3)	88.7(3)
N(5)−Os(4)−C(100)	83.2(3)	Os(4)−C(100)−Os(3)	91.1(4)
C(1)−N(2)−C(3)	110.3(8)	Os(1)−C(100)−Os(3)	89.4(3)
C(1)−N(5)−C(4)	109.1(7)	Os(5)−C(100)−Os(2)	88.5(3)
N(5)−C(1)−N(2)	105.3(7)	Os(4)−C(100)−Os(2)	91.7(3)
N(5)−C(1)−Os(1)	121.7(6)	Os(1)−C(100)−Os(2)	89.9(4)
N(2)−C(1)−Os(1)	133.0(6)	Os(3)−C(100)−Os(2)	177.1(5)
N(2)−C(3)−C(4)	107.6(8)	Os(3)−Os(4)−C(100)	43.1(2)
N(5)−C(4)−C(3)	107.7(8)	Os(2)−Os(4)−C(100)	42.8(2)

is suspected to occur by a radical intermediate.[77] This could lead to elimination of an IMes fragment as an ionic species such as $[H\text{-IMes}]^+$ on the column as previously seen in the formation of (**3**).

It is suggested that the introduction of sterically demanding NHC species into transition metal clusters could allow for their use in the breaking of metal−metal bonds to generate metal-skeletal arrangements that are difficult to synthesize by other means. The results described here suggest a role for NHCs beyond that of a simple ligand in osmium clusters, a role for which they are already known in main group chemistry.

Characterization of $[Ru_4(\mu\text{-}H)_4(CO)_{11}(n\cdot IMes)]$ (7). In the course of the analysis, $[Os_4(\mu\text{-}H)_4(CO)_{11}(n\cdot IMes)]$ (**4**) was found to be exceptionally robust. Complexes of ruthenium are generally much more labile than those of osmium;[56,58,64] thus, it was considered that the generation of a ruthenium analogue of (**4**) may be difficult under ambient conditions. Consonant with our results, Ellul et al. and Cabeza et al. have recently reported interesting results on the reaction of NHCs with the trinuclear ruthenium carbonyl, $[Ru_3(CO)_{12}]$, specifically on the activation of the backbone C(3) and C(4) positions and the activation of an organic methyl group attached to the NHC.[30,46]

Reaction of $[Ru_4(\mu\text{-}H)_4(CO)_{12}]$ under identical conditions to those used to generate (**4**) yields a single orange product (**7**) appeared to have the formula $[Ru_4(\mu\text{-}H)_4(CO)_{11}(n\cdot IMes)]$ based upon spectroscopy (Scheme 8).

Scheme 8. Reaction of $[Ru_4(\mu\text{-}H)_4(CO)_{12}]$ with [(IMes)AgCl] Using $(CH_3)_3NO$ as a Decarbonylation Agent, Producing the Proposed $[Ru_4(\mu\text{-}H)_4(CO)_{11}(IMes)]$ (7)

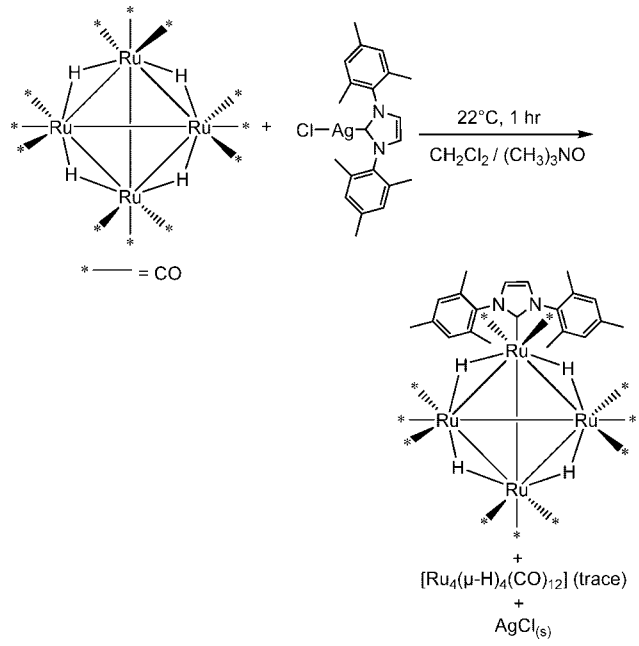

IR solution studies on (**7**) reveal seven bands in the ν(CO) region (Figure 10). The infrared band pattern is similar to that of $[Os_4(\mu\text{-}H)_4(CO)_{11}(n\cdot IMes)]$ (**4**), suggesting similar symmetry and composition.[78] The shift of the bands to lower wavenumbers relative to the osmium analogue is expected and also observed for $[Ru_3(CO)_{12}]$ vs $[Os_3(CO)_{12}]$, which have the same structural arrangement but a slight shift in IR band pattern in the ν(CO) region.[78−80]

Compound (**7**) was found to decompose at room temperature even under nitrogen atomosphere to a solid that was insoluble in dichloromethane. Lowering the temperature appeared to slow the decomposition as a sample placed in the freezer at −20 °C was found to be stable for up to one week. The brownish-red decomposition products could be readily removed by column chromatography on silica gel without causing structural alteration of (**7**) as confirmed by IR and NMR studies. Unfortunately, all attempts to identify these decomposition products were unsuccessful.

Further support for the formation of $[Ru_4(\mu\text{-}H)_4(CO)_{11}(n\cdot IMes)]$ comes in the form of ^1H NMR data, which revealed the presence of the IMes ligand and hydride signals. The broadness of the resonances at −17.76 ppm and 18.02 ppm is due to fluxional motion of the hydrides.

The $^{13}C\{^1H\}$ NMR spectrum was found to have peaks consistent with one IMes ligand and displayed a pattern similar to that observed for the osmium derivative. Additional peaks of lower intensity are believed to be due to impurities. The $^{13}C\{^1H\}$ NMR spectrum of the carbonyl region was acquired and analyzed. Three resonances were found at 188.6 ppm, 195.0 ppm, and 198.3 ppm in a relative intensity ratio of 3:7:2, though it is acknowledged that the signal with the integral of 7 may be inaccurate due to broadening. The pattern and integrals are similar to those of (**4**) observed at room temperature, although

(77) Watson, W. H.; Kandala, S.; Richmond, M. G. *J. Chem. Crystallogr.* **2006**, *36*, 71–75.

(78) Stuart, B. H. *Infrared Spectroscopy: Fundamentals and Applications*; John C. Wiley & Sons, Inc.: Hoboken, NJ, 2004.

(79) Rushman, P.; Van Buuren, G. N.; Shiralian, M.; Pomeroy, R. K. *Organometallics* **1983**, *2*, 693–694.

(80) Eady, C. R.; Johnson, B. F. G.; Lewis, J. *J. Organomet. Chem.* **1973**, *57*, C84−C86.

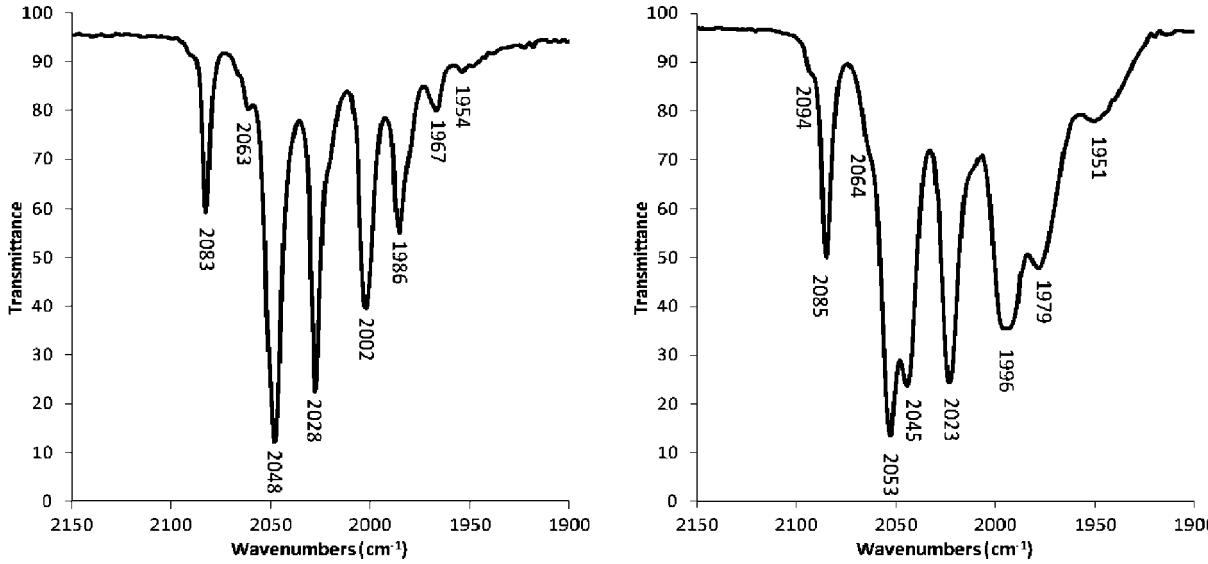

Figure 10. IR spectrum of (**7**) (left) and (**4**) (right) in CD_2Cl_2, ν(CO) region.

the resonance at 195.0 ppm for the ruthenium derivative is sharper, indicating a higher rate of fluxional motion. The resonance at 172.3 ppm is attributed to the carbenic carbon. Mass spectroscopic analysis was attempted on a solid sample of (**7**), but these were inconclusive because of decomposition; however, elemental analysis was successful and in accord with the formulation of (**7**).

The thermal instability of (**7**) is most likely the result of substituent steric strain caused by the bulky mesityl rings. The weaker metal−metal bonding in ruthenium complexes, as compared to osmium, creates conditions in which the complex is more likely to decompose under ambient conditions.[64] It is worth mentioning that attempted reaction of $[Ru_4(\mu\text{-H})_4(CO)_{12}]$ and [(IMes)AgCl] at 60 °C in toluene resulted in complete decomposition of *all* material to an insoluble black solid. While many mononuclear ruthenium−NHC complexes are known, including the second generation Grubbs catalysts, few examples of ruthenium−NHC cluster species exist.[37,41,44,46] However, a recently prepared triruthenium carbonyl complex containing an NHC ligand, 1,3-dimethylimidazol-2-ylidene (Me_2Im), was found to orient itself so as to minimize steric interactions of the methyl groups with neighboring CO ligands attached to the same ruthenium atom.[30] Given the much larger size of the 2,4,6-trimethylphenyl groups in (**7**), it is unlikely that an energetically favorable conformation exists; their interaction with the CO groups on neighboring ruthenium atoms likely causes too much steric strain.

The properties of ruthenium derivative (**7**) highlight the advantages of osmium analogues that offer greater stability. The isolation of stable osmium species, which may otherwise be unstable or persist only as postulated intermediates in ruthenium systems, has the potential to shed light on complex reaction pathways. Given the importance of ruthenium as a catalyst, the isolation of osmium species possessing novel bonding motifs is of great importance to structural transition metal chemistry and catalytic systems.

3. Reactivity of an Osmium-NHC Complex. Characterization of $\{Os_5(\mu_5\text{-C})(\mu\text{-H})(CO)_{14}[\eta\text{-C-}\eta\text{-}NC_2H_2(Mes)]\}$ (8). Thermolysis of $[Os_4(\mu\text{-H})_4(CO)_{11}(n\cdot IMes)]$ (**4**) in benzene at 200 °C yields four isolable clusters (Scheme 9). Separation of these products was achieved by silica column chromatography with elution in a dichloromethane and hexanes solvent system. The materials isolated include two clusters that contain a larger number of metal atoms than the starting material. Also, two tetranuclear clusters were isolated from the reaction mixture.

Infrared studies on a solution of (**8**) in dichloromethane show eight bands in the ν(CO) region. ^{1}H solution NMR of the yellow solid (**8**) revealed peaks consistent with the IMes ligand. However, the imidazole protons gave rise to two separate signals, at 6.31 (1H) and 7.08 ppm (1H), indicating asymmetry in the ligand. $^{13}C\{^1H\}$ solution NMR studies confirm the presence of the IMes ligand and also reveal a resonance at 377.9 ppm, the region typical for carbide ligands.[81−83] To determine atomic connectivity, X-ray crystallographic techniques were employed, and the results of the study are shown in Figure 11 with selected bond lengths and angles in Table 8.

The study revealed the presence of a pentanuclear osmium cluster with a previously observed bridged butterfly arrangement of metal atoms and a carbide atom at the center of the framework bonded to all five metal atoms.[80,81,83] The IMes ligand has undergone decomposition, losing one of its 2,4,6-trimethylphenyl rings, presumably via C−N bond activation and allowing for coordination to an osmium atom through an imidazole ring nitrogen. The osmium−carbene bond is intact. The carbide atom is believed to come from the reaction of two molecules of CO to form CO_2 and C, a known process in carbonyl chemistry, rather than originating from an organic carbon.[84,85] This belief was confirmed by ^{13}CO enrichment studies. Other mechanisms for carbide formation have been suggested including proton-induced reduction of CO, which given the loss of hydrides from (**4**), may play a role as well.[86,87] Cabeza et al. have recently communicated a structurally similar complex for a ruthenium−NHC

(81) Johnson, B. F. G.; Lewis, J.; Nelson, W. J. H.; Nicholls, J. N.; Puga, J.; Raithby, P. R.; Rosales, M. J.; Schroeder, M.; Vargas, M. D. *J. Chem. Soc., Dalton Trans.* **1983**, 2447–2457.
(82) Mason, J. *J. Am. Chem. Soc.* **1991**, *113*, 6056–6062.
(83) Eady, C. R.; Johnson, B. F. G.; Lewis, J. *J. Chem. Soc., Dalton Trans.* **1975**, 2606–2611.
(84) Bailey, P. J.; Duer, M. J.; Johnson, B. F. G.; Lewis, J.; Conole, G.; McPartlin, M.; Powell, H. R.; Anson, C. E. *J. Organomet. Chem.* **1990**, *383*, 441–461.
(85) Anson, C. E.; Bailey, P. J.; Conole, G.; Johnson, B. F. G.; Lewis, J.; McPartlin, M.; Powell, H. R. *J. Chem. Soc., Chem. Commun.* **1989**, 442–444.
(86) Whitmire, K. H.; Shriver, D. F. *J. Am. Chem. Soc.* **1981**, *103*, 6754–6755.
(87) Kolis, J. W.; Holt, E. M.; Drezdzon, M.; Whitmire, K. H.; Shriver, D. F. *J. Am. Chem. Soc.* **1982**, *104*, 6134–6135.

Scheme 9. Thermolysis of $[Os_4(\mu\text{-}H)_4(CO)_{11}(n\cdot IMes)]$ at 200 °C in Benzene, Producing $\{Os_5(\mu_5\text{-}C)(\mu\text{-}H)(CO)_{14}[\eta\text{-}C\text{-}\eta\text{-}NC_2H_2(Mes)]\}$ (8), $[Os_6(\mu\text{-}H)_4(\mu_5\text{-}C)(CO)_{15}(IMes)]$ (9), $[Os_4(\mu\text{-}H)_4(CO)_{11}(a\cdot IMes)]$ (10), and $\{Os_4(\mu\text{-}H)(CO)_{10}[(\eta\text{-}C)N(Mes)\text{-}C_2H_2NC_6H_2(CH_3)_2(\eta^2\text{-}C)(\eta\text{-}C)C_4H_4(\eta^2\text{-}C)]\}$ (11)

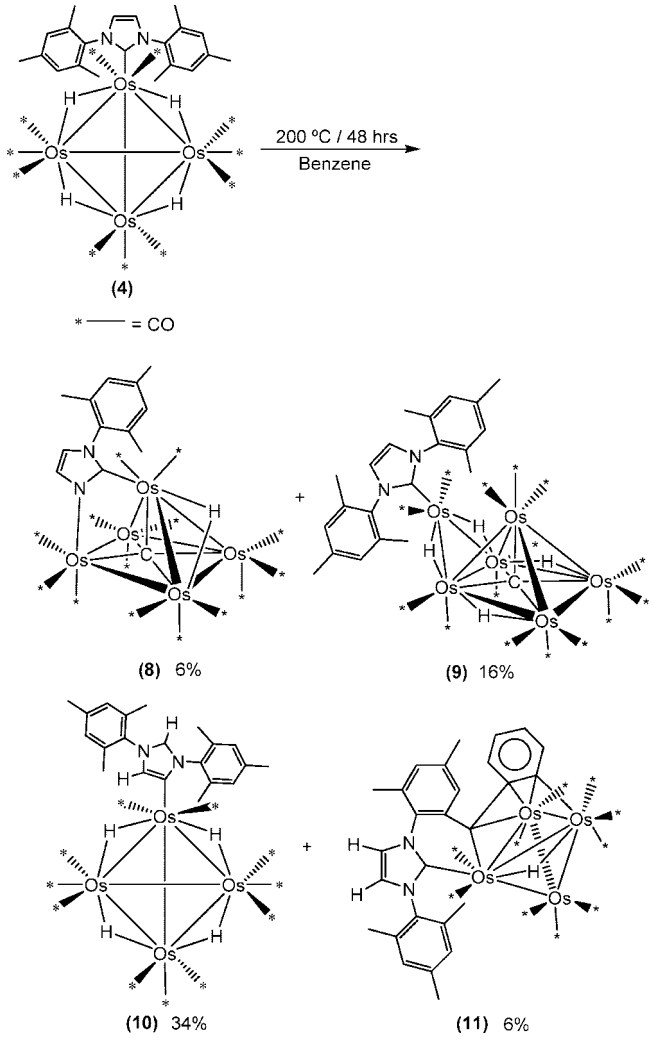

cluster under heating; however, the carbide source is attributed to carbon abstraction from an organic carbon rather than a CO molecule.[45] The difference in reactivity maybe due to the propensity for ruthenium complexes to support activating bridging ligands under milder conditions in the presence of NHCs.

Complex (**8**) is a 76-electron system, with the carbene of the IMes derived ligand acting as bidentate donor, with respect to PSEPT.[66,88] The carbene donates two electrons, and the nitrogen center provides one electron as it requires the lone pair for delocalized imidazole bonding resulting in a formal positive charge on the atom. Although NMR did not indicate that a hydride was present, X-ray data and XHYDEX analysis of the complex suggest a possible bridging site between Os(1) and Os(5). The Os(1)−Os(5) bond is the longest in the cluster at 2.9300(5) Å. In (**8**), residual electron density was localized between Os(1) and Os(5).

The metal−carbene bond, Os(1)−C(1), has a length of 2.057(8) Å, similar to others previously determined. The newly formed interaction with the imidazole ring nitrogen, Os(4)−N(5) of length

(88) Mingos, D. M. P.; Wales, D. J. *Introduction to Cluster Chemistry*; Prentice-Hall: Englewood Cliffs, NJ, 1990; pp 195−216; 250−271.

Table 8. Selected Bond Lengths and Angles for $[Os_6(\mu\text{-}H)_4(\mu_5\text{-}C)(CO)_{15}(IMes)]$ (9)

Bond Lengths (Å)			
Os(1)−Os(3)	2.7526(7)	Os(1)−C(1)	2.094(15)
Os(1)−Os(2)	2.8466(8)	C(1)−N(5)	1.350(17)
Os(2)−Os(4)	2.8369(7)	C(1)−N(2)	1.363(17)
Os(2)−Os(5)	2.8386(7)	N(2)−C(3)	1.419(18)
Os(2)−Os(3)	2.8685(7)	N(2)−C(81)	1.422(16)
Os(4)−Os(6)	2.8705(7)	C(3)−C(4)	1.35(2)
Os(4)−Os(5)	2.8884(8)	C(4)−N(5)	1.384(18)
Os(3)−Os(6)	2.8424(7)	Os(2)-C	2.039(11)
Os(3)−Os(4)	2.8862(7)	Os(3)-C	2.010(13)
Os(5)−Os(6)	2.9070(7)	Os(4)-C	2.164(11)
C(11)−O(11)	1.170(16)	Os(5)-C	2.011(12)
C(53)−O(53)	1.090(18)	Os(6)-C	2.056(11)
Bond Angles (°)			
Os(4)−Os(2)−Os(5)	61.183(19)	Os(1)−Os(3)−Os(4)	68.781(19)
Os(1)−Os(3)−Os(6)	128.92(2)	Os(6)−Os(3)−Os(4)	60.138(17)
Os(4)−Os(2)−Os(1)	68.21(2)	Os(3)−Os(6)−Os(4)	60.688(17)
Os(5)−Os(2)−Os(1)	128.69(2)	Os(3)−Os(6)−Os(5)	88.63(2)
Os(4)−Os(2)−Os(3)	60.774(18)	Os(4)−Os(6)−Os(5)	59.987(18)
Os(5)−Os(2)−Os(3)	89.47(2)	Os(3)−C-Os(5)	174.9(7)
Os(1)−Os(2)−Os(3)	57.583(18)	Os(3)−C-Os(2)	90.2(5)
Os(3)−Os(1)−Os(2)	61.608(19)	Os(5)−C-Os(2)	89.0(5)
Os(2)−Os(5)−Os(4)	59.380(18)	Os(3)−C-Os(6)	88.7(5)
Os(2)−Os(3)−Os(4)	59.072(17)	Os(5)−C-Os(6)	91.2(5)
Os(2)−Os(4)−Os(6)	91.29(2)	Os(2)−C-Os(6)	170.5(6)
Os(2)−Os(4)−Os(3)	60.154(18)	Os(3)−C-Os(4)	87.4(5)
Os(6)−Os(4)−Os(3)	59.174(17)	Os(5)−C-Os(4)	87.5(4)
Os(2)−Os(5)−Os(6)	90.50(2)	Os(2)−C-Os(4)	84.9(4)
Os(4)−Os(5)−Os(6)	59.378(17)	Os(6)−C-Os(4)	85.7(4)
Os(1)−Os(3)−Os(2)	60.809(19)	N(5)−C(1)−N(2)	105.8(13)
Os(6)−Os(3)−Os(2)	91.22(2)	N(5)−C(1)−Os(1)	126.6(11)
Os(2)−Os(4)−Os(5)	59.437(18)	N(2)−C(1)−Os(1)	127.3(10)
Os(6)−Os(4)−Os(5)	60.634(18)	C(1)−N(2)−C(3)	109.6(12)
Os(3)−Os(4)−Os(5)	88.15(2)	C(4)−C(3)−N(2)	106.1(14)

2.113(7) Å, is consistent with that recently reported by Sinha et al. for the mononuclear complex $[Os(H)(CO)(PPh_3)_2(PyaiH_2)]$ ($PyaiH_2$ = 2-{3′-(pyridylazo)}imidazole) with an imidazole nitrogen−osmium bond length of 2.101(3) Å.[38]

The $^{13}C\{^1H\}$ NMR spectrum of the carbonyl region reveals eight resonances consistent with the structure of (**8**). The appearance of eight resonances of the expected intensity confirms that the carbonyl structure of this complex is static at this temperature and that no fluxional motion of the carbonyls is occurring.

Characterization of $[Os_6(\mu\text{-}H)_4(\mu_5\text{-}C)(CO)_{15}(IMes)]$ (9). $[Os_6(\mu\text{-}H)_4(\mu_5\text{-}C)(CO)_{15}(IMes)]$ (**9**) was isolated from the thermolysis of $[Os_4(\mu\text{-}H)_4(CO)_{11}(n\cdot IMes)]$ (**4**) (Scheme 9). Infrared studies on a solution of (**9**) in dichloromethane showed seven bands in the ν(CO) region. LSIMS analysis revealed a molecular ion of m/z 1881.8, suggesting a hexanuclear osmium species. ^1H solution NMR confirmed the presence of an IMes ligand as well as showing four hydride resonances.

Suitable crystals of (**9**) grown from a concentrated solution in dichloromethane and hexanes were subjected to X-ray diffraction analysis, and the results are shown in Figure 12 with selected bond lengths and angles in Table 8.

The results of the study show a hexanuclear edge-bridged square pyramidal cluster. The base of the square pyramid contains a carbide atom similar to (**8**). Coordination of the osmium atoms is fulfilled by 15 terminal carbonyl ligands. The positions of the hydride ligands were determined by the XHYDEX program with the resulting positions integrated into the crystal data.[52] There were two hydride atoms in the basal plane and two hydrides spanning the edge bridging metal−metal bonds.

Comparison of the metal−metal bonds with those in (**8**) reveals similar bond lengths between the apical atom of the

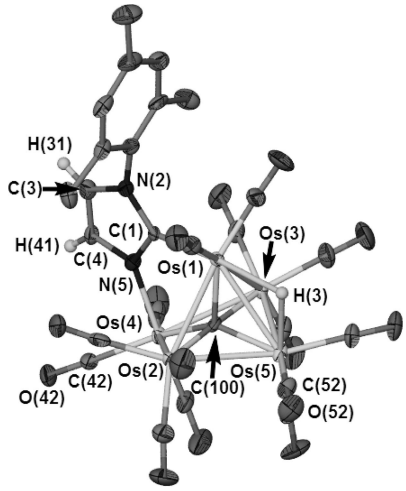

Figure 11. ORTEP view of $[Os_5(\mu_5\text{-}C)(\mu\text{-}H)(CO)_{14}(\eta\text{-}C\text{-}\eta\text{-}N\text{-}C_2H_2(Mes)]$ (**8**). Ellipsoids are drawn at the 50% probability level. 2,4,6-Trimethylphenyl hydrogens have been omitted for clarity.

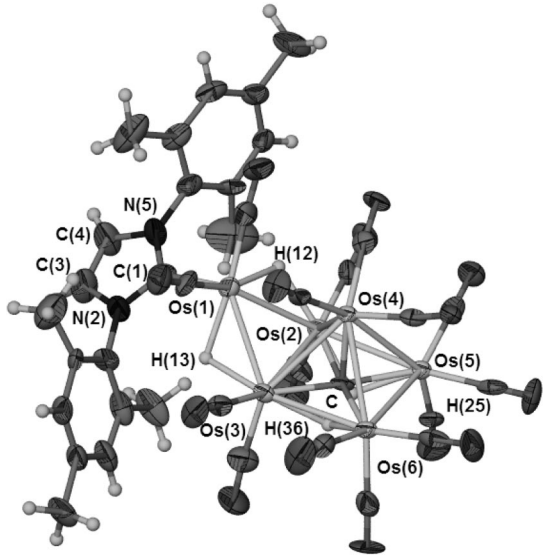

Figure 12. ORTEP view of $[Os_6(\mu\text{-}H)_4(\mu_5\text{-}C)(CO)_{15}(IMes)]$ (**9**). Ellipsoids are drawn at the 50% probability level.

pyramid and those that form the base. The average length of these bonds is 2.871(7) Å in (**9**) and 2.887(5) Å in (**8**). The bonds at the base of the pyramid average to 2.864(7) Å in (**9**) compared to 2.899(5) Å in (**8**).

Examination of the osmium−carbide distances reveal an average of 2.0549(12) Å for the atoms that lie at the base of the pyramid and a longer length of 2.164(11) Å to the apical metal. Similar values were found for (**8**).

The $^{13}C\{^1H\}$ NMR shows the carbide resonance at 353.8 compared 377.9 ppm in (**8**). Similar to (**8**), the carbide acts as a four-electron donor, exerting no influence on the periphery and thereby allowing the four electrons to be added without the requirement of additional ligands, which would cause steric crowding, thus stabilizing (**9**).[81]

The $^{13}C\{^1H\}$ NMR spectrum of the carbonyl region reveals seven resonances consistent with the structure of (**9**). The relative peak intensities are those expected for a molecule containing a mirror plane bisecting the molecule, and therefore, the hydrides must be arranged symmetrically. The seven unique carbonyl resonances are observed in a 2:2:2:2:2:2:3 intensity pattern. Their complete assignment is not possible with the exception

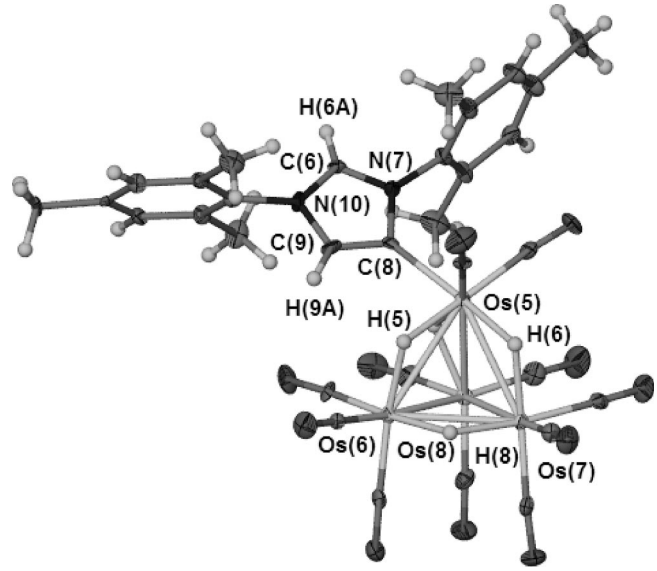

Figure 13. ORTEP view of $[Os_4(\mu\text{-}H)_4(CO)_{11}(a\cdot IMes)]$ (**10**). Ellipsoids are drawn at the 50% probability level.

of those attached to the apical osmium atom on the square pyramid. These carbonyls are undergoing fluxional rotation about the metal; therefore, their resonance is broad.[74]

Characterization of $[Os_4(\mu\text{-}H)_4(CO)_{11}(a\cdot IMes)]$ (10). The major product of the thermolysis was isolated as a yellow band eluted following column chromatography. Recrystallization was achieved from a concentrated solution of dichloromethane and yielded yellow crystals of (**10**) similar in appearance to (**4**).

IR solution studies on (**10**) in dichloromethane reveal a band pattern very similar to that of (**4**). Comparison of the infrared spectrum of (**4**) to that of (**10**) shows a 1 to 2 cm^{-1} shift to lower wavenumbers in (**10**).

For this study, the resolution of the IR instrument was set to 1 cm^{-1} to ascertain that the shift was real and not the result of instrument limitations. These data suggest that the $[Os_4(\mu\text{-}H)_4(CO)_{11}]$ core has been maintained.

The ^1H NMR data of (**10**) were different from that of (**4**). For instance, three distinct signals in a 1:2:1 pattern were observed in the anticipated region for osmium hydrides rather than the single resonance in (**4**).[54] Also, there are five signals with an integration corresponding to 18H for the 2,4,6-trimethylphenyl CH_3 groups, indicating a significant lowering of symmetry for the IMes ligand. Mass spectral data and elemental analysis indicated that the solid was indeed an isomer of (**4**).

Crystals of (**10**) were grown from a concentrated CH_2Cl_2 solution and subjected to X-ray diffraction analysis. The study determined that there were two crystallographically unique and structurally similar molecules in the unit cell, and the structures are shown in Figure 13, with selected bond lengths and angles shown in Table 9. Indeed, (**10**) is an isomer of (**4**). Hydride positions and potential energies were found using XHYDEX, and the resulting positions were integrated into the crystal data. Thus, returning to the IR data, it can be concluded that the abnormal carbene is slightly more electron-donating than the normal isomer, as is suggested by the slight lowering of the CO stretches.[37]

The structure of (**10**) contains an IMes ligand bound to an osmium cluster, with a single carbon−osmium bond, C(3)−Os(1), which is 2.121(12) Å long compared to the length of Os(1)−C(1) 2.05(8) Å in (**4**). In the cluster, osmium−osmium bonds supporting bridging hydrides were found to range from 3.0309(7)

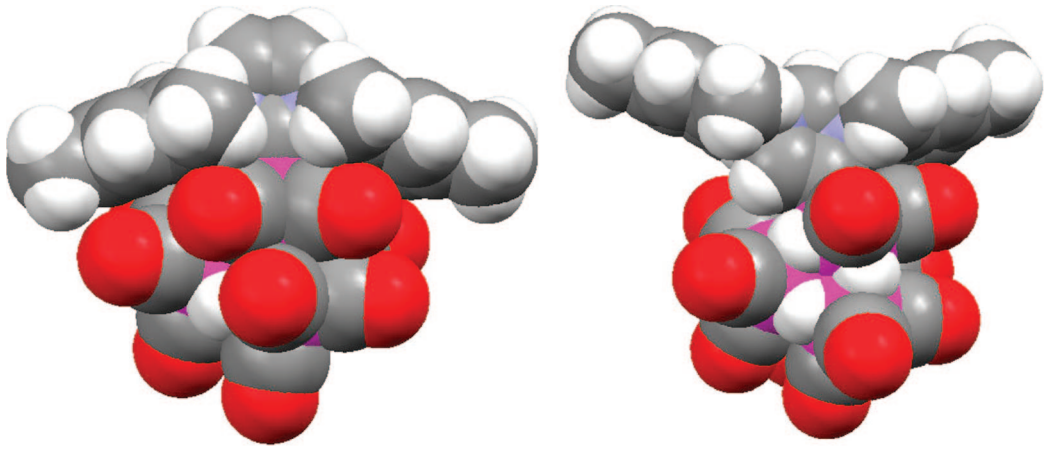

Figure 14. Space filling models of the normal (**4**) (left) and abnormal (**9**) (right) complexes illustrate the effect of steric crowding at the location of carbene bonding.

Table 9. Selected Bond Lengths and Angles for $[Os_4(\mu\text{-}H)_4(CO)_{11}(a\cdot IMes)]$ (9)

Bond Lengths (Å)			
Os(5)−Os(7)	2.9882(7)	C(9)−N(10)	1.367(17)
Os(5)−Os(8)	2.9935(7)	Os(5)−H(5)	1.79(4)
Os(5)−Os(6)	3.0142(7)	Os(5)−H(6)	1.79(4)
Os(6)−Os(8)	2.8069(7)	Os(5)−H(7)	1.78(4)
Os(6)−Os(7)	2.9307(7)	Os(6)−H(5)	1.79(4)
Os(7)−Os(8)	2.8166(7)	Os(6)−H(8)	1.79(4)
C(6)−N(7)	1.315(17)	Os(7)−H(6)	1.79(4)
C(6)−N(10)	1.327(16)	Os(7)−H(8)	1.78(4)
N(7)−C(8)	1.431(16)	Os(8)−H(7)	1.79(4)
C(8)−C(9)	1.333(19)	Os(5)−C(8)	2.095(13)

Bond Angles (°)			
Os(7)−Os(5)−Os(8)	56.181(16)	Os(7)−Os(8)−Os(5)	61.815(17)
Os(7)−Os(5)−Os(6)	58.450(16)	N(7)−C(6)−N(10)	108.0(11)
Os(8)−Os(5)−Os(6)	55.708(16)	C(6)−N(7)−C(8)	110.9(10)
Os(8)−Os(6)−Os(7)	58.752(17)	C(9)−C(8)−N(7)	101.8(11)
Os(8)−Os(6)−Os(5)	61.772(16)	C(9)−C(8)−Os(5)	128.9(10)
Os(7)−Os(6)−Os(5)	60.332(16)	N(7)−C(8)−Os(5)	129.3(9)
Os(8)−Os(7)−Os(6)	58.430(17)	C(8)−C(9)−N(10)	111.8(12)
Os(8)−Os(7)−Os(5)	62.003(17)	C(6)−N(10)−C(9)	107.5(11)
Os(6)−Os(7)−Os(5)	61.218(17)	C(8)−Os(5)−Os(7)	152.3(3)
Os(6)−Os(8)−Os(7)	62.819(18)	C(8)−Os(5)−Os(6)	95.4(3)
Os(6)−Os(8)−Os(5)	62.520(17)		

Å to 2.9235(7) Å compared to a range of 2.990(2) Å to 2.938(2) Å in (**4**). Osmium−osmium distances without hydride ligands were found to range from 2.8177(7) Å to 2.8126(7) Å, clearly differentiating them from hydride-supporting bonds.[65,69,70] Osmium−hydride distances were refined and found to be 1.76(4) Å. M−C−O angles in (**10**) range from 172.6(12)° to 179.6(14)° comparable to those found in (**4**). Other metrical parameters such as the tetrahedral metal skeletal bond angles are similar to those of (**4**).

It can be seen that (**10**) has a C_s type geometry in the solid state structure, suggested by the 1:2:1 relative intensity of the hydride resonances in the ^{1}H NMR in solution.[70,71]

A ^{13}C-enriched sample of (**10**) was prepared and the $^{13}C\{^1H\}$ NMR spectrum acquired at 25 and 5 °C in CD_2Cl_2. The observation of broadened resonances indicates that not all the carbonyls are rigid on the NMR time scale at 25 and 5 °C. The observation of two sharp resonances at 177.4 ppm and 177.8 ppm is likely due to axial carbonyl ligands.[74,75,89] The four sharp resonances at 170.4 ppm, 171.0 ppm, 171.5 ppm, and 171.9 ppm are likely due to equatorial carbonyls, which are known to appear upfield of those of axial carbonyls.[74,75,89]

Abnormal carbenes make up a very small percentage of the known carbene complexes, approximately 2%.[37] However, it is believed that number may actually be much higher as many of the NHC metal complexes generated for use as catalysts and used *in situ* lack rigorous characterization of the active species.[37]

More to the point, while ruthenium−NHC complexes are widely studied well-known catalysts, only recently has the synthesis of an abnormal carbene cluster complex been reported. 1,3-Di-*tert*-utylimidazol-2-ylidene (I*t*Bu) reacts with $[Ru_3(CO)_{12}]$ at room temperature to generate a novel abnormal NHC−ruthenium complex.[46] This is believed to be the first example of abnormal NHC formation from a *free* monodentate carbene. Subsequent heating of this complex results in activation of the second abnormal (C5) site to afford a triruthenium cluster containing an Ru_3C_2 framework.[46] As previously mentioned, osmium−NHC complexes are quite rare, and (**10**) is believed to be the only known abnormal carbene complex of osmium.[37]

Most of the limited knowledge of abnormal carbenes involves iridium complexes.[37] From these studies, it has been surmised that formation of the abnormal carbene may be favored as it lowers the steric strain at the metal center. On this basis, it is noted that perhaps the conversion of (**4**) to (**10**) is not entirely unexpected since the steric constraints (steric pressure) are dramatically decreased upon isomerization from the cramped pocket around C_1 to the more spacious pocket around C_4-C_3 as shown by the space filling models (Figure 14).

The electronic effects seen in other abnormal carbenes mirror the results found here. Chiefly, abnormally bound carbenes are more electron-donating than normal carbenes on the basis of ν(CO) stretching observed in IR spectroscopy.[10,21,22,37] Also, abnormal carbene complexes can be identified by the difference in chemical shifts between the two heterocyclic protons in ^{1}H NMR spectra (>1 ppm in abnormal carbenes compared with <1 ppm in normal carbenes).[37]

The imidazole ring hydrogens are not limited to the formation of abnormal carbenes. Herrmann et al. have osmylated the NHC backbone upon treatment of $[M(CO)_5(C\{NMeCH\}_2]$ (M = Cr, Mo, W) with osmium tetraoxide leading to the formation of two new osmium−carbon interactions with the imidazole carbons.[90]

Given the extremely limited number of examples of abnormally bound carbenes that exist for comparison, the direct conversion of (**4**) to (**10**) sheds light on the nature of their

(89) Johnson, B. F. G.; Lewis, J.; Reichert, B. E.; Schorpp, K. T. *J. Chem. Soc., Dalton Trans.* **1976**, 1403–4.

(90) Herrmann, W. A.; Roesky, P. W.; Elison, M.; Artus, G.; Oefele, K. *Organometallics* **1995**, *14*, 1085–6.

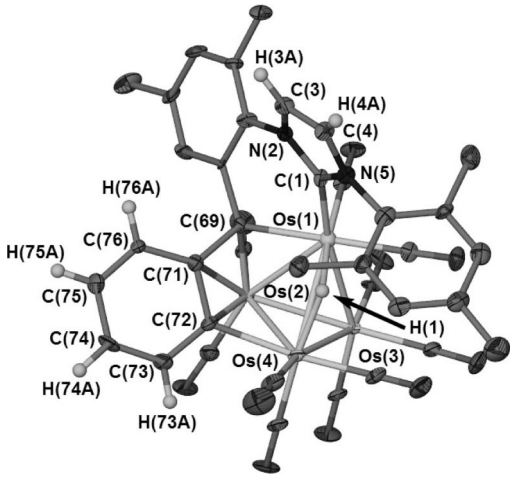

Figure 15. ORTEP view of $\{Os_4(\mu\text{-H})(CO)_{10}[(\eta\text{-C})N(Mes)C_2H_2NC_6H_2(CH_3)_2(\eta^2\text{-C})(\eta\text{-C})C_4H_4(\eta^2\text{-C})]\}$ (**11**). Ellipsoids are drawn at the 50% probability level. 2,4,6-Trimethylphenyl hydrogens have been omitted for clarity.

generation, providing a starting point for the targeted synthesis of this class of NHCs. We suggest that it is unwise to assume that NHCs bind via the C1-atom for a complex or a catalyst in which the NHC is generated *in situ* (as is the case with [(IMes)AgCl]). [(IMes)AgCl] is convenient for carbene generation because it is air- and moisture-stable, but rigorous characterization of the resulting products is required to be certain of their identity.

Characterization of $\{Os_4(\mu\text{-H})(CO)_{10}[\eta\text{-C})N(Mes)C_2H_2NC_6H_2(CH_3)_2(\eta^2\text{-C})(\eta\text{-C})C_4H_4(\eta^2\text{-C})]\}$ (11). The second tetranuclear metal complex isolated from the thermolysis of (**4**) was $\{Os_4(\mu\text{-H})(CO)_{10}[(\eta\text{-C})N(Mes)C_2H_2NC_6H_2(CH_3)_2(\eta^2\text{-C})(\eta\text{-C})C_4H_4(\eta^2\text{-C})]\}$ (**11**), isolated as a red−brown air-stable solid following column chromatography (Scheme 9). X-ray diffraction quality crystals were grown by slow evaporation from a concentrated mixture of dichloromethane and hexanes under a stream of nitrogen. The infrared spectrum of (**11**) shows seven bands in the ν(CO) region.

^{1}H NMR studies revealed the presence of five distinct signals in the region anticipated for methyl groups with an integration of 15 H compared to the 18 H expected for the IMes ligand. Furthermore, in the metal hydride region, a single resonance at −19.9 ppm indicated the presence of one unique bridging hydride ligand.[54] Curiously, new peaks were evident in the aryl region of the ^{1}H spectrum with an ABCD spin system, consistent with the incorporation of a 1,2-disubstituted benzene ring into the unit.

An X-ray crystallographic study was completed on a crystal of (**11**), and the result is shown in Figure 15, with selected bond lengths and angles shown in Table 10.

The structure of (**11**) was unanticipated; however, the elemental analysis and LSIMS (M^+ 1419.7 *m/z*) are consistent with the formulation. The complex exhibits an $Os_4(CO)_{10}$ core with an NHC ligand coordinated to one osmium site with an Os(1)−C(1) bond interaction that is 2.090(9) Å long. This is similar in length to those found in the other osmium−NHC complexes. The single bridging hydride between Os(1) and Os(4) was located by the use of XHYDEX, the longest metal−metal bond in the cluster.[52] Other osmium−osmium bond lengths range from 2.6324(5) Å to 2.8820(5) Å.

Comparison to the parent cluster (**4**) reveals that (**11**) has closed up considerably. In part, this can be attributed to the loss of the bridging hydride ligands. Further contraction can be attributed to the coordination of the former methyl group carbon with the fragment derived from benzene, which places constraints on the molecule to allow for favorable orbital overlaps.

Table 10. Selected Bond Lengths and Angles for $\{Os_4(\mu\text{-H})(CO)_{10}[(\eta\text{-C})N(Mes)C_2H_2NC_6H_2(CH_3)_2(\eta^2\text{-C})(\eta\text{-C})C_4H_4(\eta^2\text{-C})]\}$ (11)

Bond Lengths (Å)			
Os(1)−C(1)	2.090(9)	Os(1)−Os(2)	2.7608(5)
Os(1)−C(69)	2.093(10)	Os(1)−Os(3)	2.8633(5)
Os(2)−C(69)	2.199(10)	Os(1)−Os(4)	2.9045(5)
Os(2)−C(72)	2.241(10)	Os(2)−Os(3)	2.6324(5)
Os(2)−C(71)	2.365(10)	Os(2)−Os(4)	2.8038(5)
Os(4)−C(72)	2.185(10)	Os(3)−Os(4)	2.8820(5)
Os(1)−H(1)	1.74(6)	C(69)−C(71)	1.428(14)
Os(4)−H(1)	1.74(6)	C(71)−C(76)	1.409(14)
C(1)−N(2)	1.340(12)	C(71)−C(72)	1.460(13)
C(1)−N(5)	1.346(12)	C(72)−C(73)	1.428(15)
N(2)−C(3)	1.393(12)	C(73)−C(74)	1.348(16)
C(3)−C(4)	1.332(14)	C(74)−C(75)	1.441(15)
C(42)−O(42)	1.106(13)	C(75)−C(76)	1.337(15)
C(41)−O(41)	1.149(13)		

Bond Angles (°)			
Os(2)−Os(1)−Os(3)	55.781(12)	N(2)−C(1)−N(5)	104.3(8)
Os(2)−Os(1)−Os(4)	59.262(13)	N(2)−C(1)−Os(1)	124.8(7)
Os(3)−Os(1)−Os(4)	59.951(12)	N(5)−C(1)−Os(1)	130.8(7)
Os(3)−Os(2)−Os(1)	64.081(13)	C(71)−C(69)−C(66)	116.5(8)
Os(3)−Os(2)−Os(4)	63.940(14)	C(76)−C(71)−C(69)	124.2(9)
Os(1)−Os(2)−Os(4)	62.922(13)	C(76)−C(71)−C(72)	118.3(9)
Os(2)−Os(3)−Os(1)	60.138(13)	C(69)−C(71)−C(72)	116.9(9)
Os(2)−Os(3)−Os(4)	60.921(13)	C(73)−C(72)−C(71)	116.7(9)
Os(1)−Os(3)−Os(4)	60.734(12)	C(74)−C(73)−C(72)	122.2(10)
Os(2)−Os(4)−Os(3)	55.139(13)	C(73)−C(74)−C(75)	120.4(10)
Os(2)−Os(4)−Os(1)	57.816(12)	C(76)−C(75)−C(74)	119.0(10)
Os(3)−Os(4)−Os(1)	59.315(12)	C(75)−C(76)−C(71)	123.2(9)

During the thermolysis reaction, one of the methyl groups of the NHC was activated such that all three C−H bonds were cleaved. The formerly methyl carbon center now bridges two osmium sites, forming two distinct Os−C interactions: Os(1)−C(69) and Os(2)−C(69). The activation of three C−H bonds on an NHC supported complex is unprecedented and indicates that the anticipated enhanced reactivity can be achieved using metal cluster compounds.

The complex exhibits notable features including the formation of new bonds to a fragment derived from benzene (solvent). Three new osmium−carbon bonds result from this coupling: Os(2)−C(71) 2.365(10) Å, Os(2)−C(72) 2.241(10) Å, and Os(4)−C(72) 2.185(10) Å. Formation of this coupling could result from a systematic C−H bond activation of the benzene ring followed by complexation of an aromatic double bond or from a double dehydrogenation to produce a benzyne-type intermediate. However, no mechanistic pathway can be deduced from the product structure. The ring derived from benzene exhibits bond alternation, the bonds C(75)−C(76) and C(73)−C(74) have lengths of 1.337(15) Å and 1.348(16) Å, respectively, but strong shielding of one of the methyl groups on the IMes fragment indicates that the moiety exhibits a shielding cone, suggestive of aromaticity within the deformed C_6 ring. The bond between C(71)−C(72) is the longest in the former benzene molecule and is consistent in length with a single bond. It is likely somewhat deformed by its coordination to the osmium atoms and maybe lengthened as a result of electron donation into the π^* orbital of the double bond. The remaining bonds lengths in the ring between C(71)−C(76), C(75)−C(74), and C(72)−C(73) appear to be consistent with single bonds.

Finally, a C−C bond formation reaction has occurred, coupling the dehydrogenated methyl group of IMes and the dehydrogenated benzene fragment [C(69)−C(71) 1.428(14) Å]. The result of the dehydrogenation and subsequent coupling of

Scheme 10. Thermolysis of $[Os_4(\mu\text{-}H)_4(CO)_{11}(n\cdot IMes)]$ (4) at 200 °C in Toluene, Producing $\{Os_5(\mu_5\text{-}C)(CO)_{14}[\eta\text{-}C\text{-}\eta\text{-}NC_2H_2(Mes)]\}$ (8), $[Os_6(\mu\text{-}H)_4(\mu_5\text{-}C)(CO)_{15}(IMes)]$ (9), $[Os_4(\mu\text{-}H)_4(CO)_{11}(a\cdot IMes)]$ (10), and $\{Os_4(\mu\text{-}H)(CO)_{10}[(\eta\text{-}C)N(Mes)C_2H_2NC_6H_2(CH_3)_2(\eta^2\text{-}C)(\eta\text{-}C)CHC(CH_3)C_2H_2(\eta^2\text{-}C)]\}$ (12)

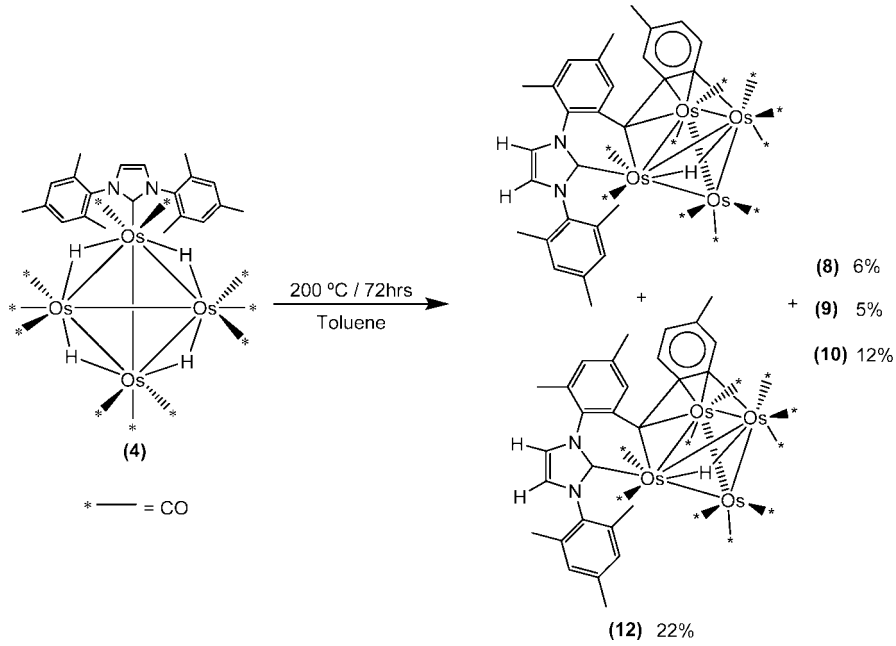

the NHC−methyl group and the benzene fragment result in formal conversion of C(69) from a methyl group to a bridging carbene. The Os(1)−C(69) 2.093(10) Å bond length is comparable to that of Os(1)−C(1). This establishes a six-membered metallacycle with the NHC group and Os(1). When viewed from the side, the chain of atoms formed by C(69)−C(71)−C(76)−C(75)−C(74)−C(73)−C(72) lie in a planar environment, a condition associated with aromaticity. It is possible that the delocalized π-system above the planar arrangement is responsible for the shielding experienced by the IMes methyl group.

Mass spectroscopic studies were completed on a sample of the reaction solvent, which had been vacuum-transferred from the remaining solid, in an attempt to determine the fate of the lost hydrogen atoms and to establish if any reduction of benzene to a 1,4-hexadiene-type molecule had occurred. Our studies only revealed the presence of benzene. The fate of the hydrogens is believed to be as released as $H_{2(g)}$, although detection of the gas from the reaction vessel could not be accomplished because of the technical difficulty associated with this. It is acknowledged that only volatile compounds would be transferred under vacuum leaving larger macrocycles and polyphenyl aromatic compounds. We note this here because of an intriguing experimental result observed in one experiment. Following elution of the colored metal complexes, the silica column was flushed with acetone and the washings collected. Following slow evaporation of this solution, a small amount (<10 mg) of a clear colorless crystalline material was recovered. X-ray diffraction studies on the solid crystalline material identified it as hexaphenylbenzene, clearly suggesting multiple dehydrogenation pathways.[91]

In order to study the reactivity of $[Os(\mu\text{-}H)_4(CO)_{11}(a\cdot IMes)]$ (**9**), a small sample (45 mg, 0.033 mmol), was thermolyzed at 200 °C in benzene (20 mL). After 48 h, the reaction mixture was then subjected to column chromatography. The isolated materials corresponded to (**11**) (23 mg, 0.016 mmol) and a trace of (**9**). Infrared spectroscopic evidence for the generation of a small amount of $[Os_4(\mu\text{-}H)_4(CO)_{12}]$ was also obtained, as indicated by the diagnostic bands at 2067 and 2019 cm^{-1}. Some insoluble black material was noted at the top of the column. It is important to note that no normal carbene isomer was observed.

The ability of both the normal and abnormal osmium−carbene species to form (**11**) suggests that rearrangement is prevalent at high temperatures. Abnormal and normal species may exist in an equilibrium at elevated temperatures mediated by reversible intramolecular rearrangement of a hydrogen atom within the imidazole ring.

Characterization of $\{Os_4(\mu\text{-}H)(CO)_{10}[\eta\text{-}C)N(Mes)C_2H_2NC_6H_2(CH_3)_2(\eta^2\text{-}C)(\eta C)CHC(CH_3)C_2H_2(\eta^2\text{-}C)]\}$ (12). Following isolation of (**11**), which contained a fragment derived from the solvent (benzene), the reaction was repeated in toluene (Scheme 10). Using the same preparative method as discussed in the previous section, clusters (**8**), (**9**), and (**10**) were isolated from the reaction mixture following chromatography and then identified by NMR and IR analysis. The new complex, $\{Os_4(\mu\text{-}H)(CO)_{10}[(\eta\text{-}C)N(Mes)C_2H_2NC_6H_2(CH_3)_2(\eta^2\text{-}C)(\eta\text{-}C)CHC(CH_3)C_2H_2(\eta^2\text{-}C)]\}$ (**12**), was isolated as a brown band from the column, and X-ray quality crystals were grown from a concentrated solution of hexanes and dichloromethane at −20 °C.

Infrared studies displayed a band pattern comparable to that of (**11**) with only a slight shift in peak positions. LSIMS analysis gave a molecular ion of *m*/*z* 1433.9, the expected mass of a complex analogous to (**11**). ^1H solution NMR of (**12**) revealed a pattern in the methyl region similar to that of (**11**), but this suggested that there were regioisomers present. The highly shielded resonances at 1.36 ppm and 1.37 ppm, with each signal integrating to three protons, as well as signals at 2.36 and 2.37 ppm with similar integrations were present. Examination of the hydride region also showed two resonances.[54] To determine atomic connectivity an X-ray diffraction was completed, and the results are shown in Figure 16 with selected bond lengths and angles presented in Table 11. *In toto*, the evidence suggests that the brown solid is composed of two compounds that are regioisomers of each other formed in a 50:50 ratio.

(91) Bart, J. C. J. *Acta Crystallopgr., Sect. B* **1968**, *24*, 1277–1287.

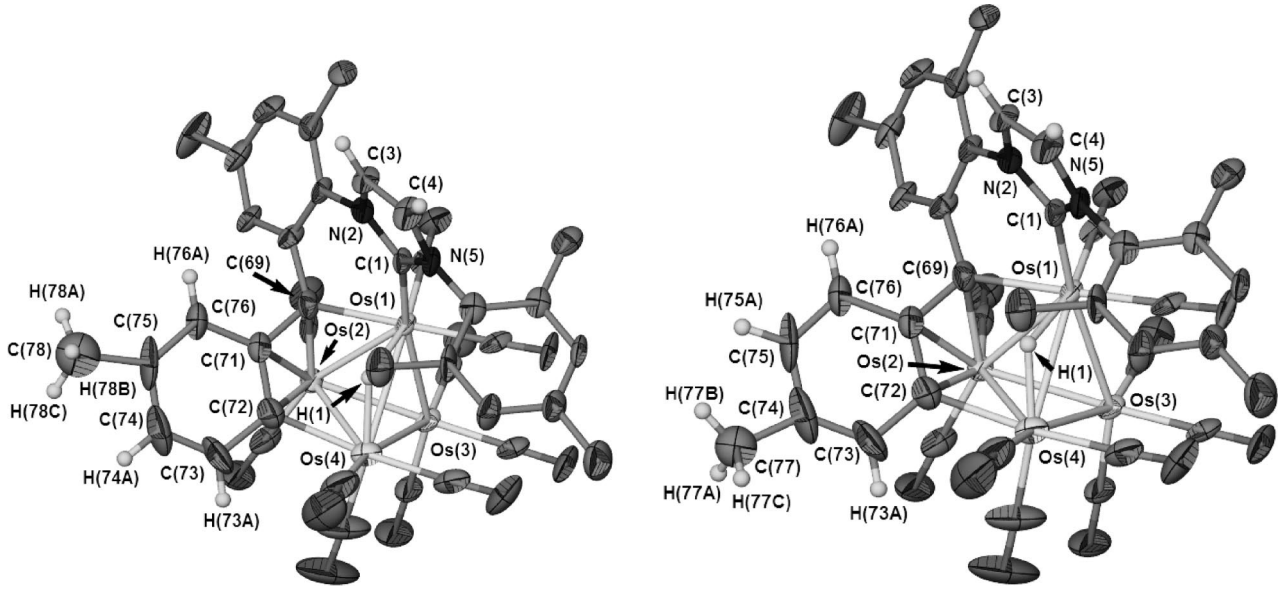

Figure 16. ORTEP view of $\{Os_4(\mu\text{-H})(CO)_{10}[(\eta\text{-C})N(Mes)C_2H_2NC_6H_2(CH_3)_2(\eta^2\text{-C})(\eta\text{-C})CHC(CH_3)C_2H_2(\eta^2\text{-C})]\}$ (**12**). Ellipsoids are drawn at the 50% probability level. 2,4,6-Trimethylphenyl hydrogens have been omitted for clarity. The methyl group of the toluene was disordered over two sites. The methyl group was refined isotropically at half-occupancy. Of the four possible sites of addition, only two were observed.

Table 11. Selected Bond Lengths and Angles for $\{Os_4(\mu\text{-H})(CO)_{10}[(\eta\text{-C})N(Mes)C_2H_2NC_6H_2(CH_3)_2(\eta^2\text{-C})(\eta\text{-C})CHC(CH_3)C_2H_2(\eta^2\text{-C})]\}$ (12)

Bond Lengths (Å)			
Os(1)−C(1)	2.062(10)	C(69)−C(71)	1.450(16)
Os(1)−C(69)	2.094(12)	C(71)−C(72)	1.415(17)
Os(2)−C(69)	2.217(11)	C(71)−C(76)	1.465(17)
Os(2)−C(72)	2.227(13)	C(72)−C(73)	1.439(17)
Os(2)−C(71)	2.377(11)	C(73)−C(74)	1.37(2)
Os(4)−C(72)	2.192(14)	C(74)−C(75)	1.45(2)
Os(1)−Os(2)	2.7597(6)	C(74)−C(77)	1.48(3)
Os(1)−Os(3)	2.8569(6)	C(75)−C(76)	1.36(2)
Os(1)−Os(4)	2.9049(6)	C(75)−C(78)	1.54(4)
Os(2)−Os(3)	2.6326(7)	C(1)−N(2)	1.362(13)
Os(2)−Os(4)	2.7930(7)	C(1)−N(5)	1.372(14)
Os(3)−Os(4)	2.8725(7)	N(2)−C(3)	1.430(13)
Os(1)−H(1)	1.69(6)	C(3)−C(4)	1.355(17)
Os(4)−H(1)	1.69(6)	C(4)−N(5)	1.410(14)
C(31)−O(31)	1.184(13)	C(41)−O(41)	1.123(16)
Bond Angles (°)			
Os(2)−Os(1)−Os(3)	55.869(16)	C(71)−C(69)−C(66)	118.0(10)
Os(2)−Os(1)−Os(4)	59.018(17)	C(72)−C(71)−C(69)	119.1(11)
Os(3)−Os(1)−Os(4)	59.802(16)	C(72)−C(71)−C(76)	122.1(11)
Os(3)−Os(2)−Os(1)	63.934(16)	C(69)−C(71)−C(76)	118.2(11)
Os(3)−Os(2)−Os(4)	63.855(19)	C(74)−C(73)−C(72)	119.1(16)
Os(1)−Os(2)−Os(4)	63.083(17)	C(73)−C(74)−C(75)	121.7(14)
Os(2)−Os(3)−Os(1)	60.198(16)	C(73)−C(74)−C(77)	134(2)
Os(2)−Os(3)−Os(4)	60.790(19)	C(75)−C(74)−C(77)	104(2)
Os(1)−Os(3)−Os(4)	60.929(16)	C(76)−C(75)−C(74)	121.5(14)
Os(2)−Os(4)−Os(3)	55.355(17)	C(76)−C(75)−C(78)	132(2)
Os(2)−Os(4)−Os(1)	57.899(15)	C(74)−C(75)−C(78)	106.0(19)
Os(3)−Os(4)−Os(1)	59.269(15)	C(75)−C(76)−C(71)	116.9(14)
N(2)−C(1)−N(5)	104.1(9)	N(5)−C(1)−Os(1)	131.0(8)
N(2)−C(1)−Os(1)	124.5(8)		

The structure of (**12**) was analogous to that of (**11**). However, the reaction displayed regioselectivity. The two structures formed in a 1:1 ratio differed only in the orientation of the toluene-dervied methyl groups. In light of this disorder, the methyl group of the toluene was refined isotropically with 50% occupancy. Thus, the disorder was responsible for the appearance of the extra peaks previously observed in the NMR data. The elemental analysis is consistent with the formulation presented.

The complex exhibits an $Os_4(CO)_{10}$ core with an NHC ligand coordinated to one osmium site with an Os(1)−C(1) bond that is 2.062(10) Å long, comparable to (**11**) and similar in length to those found in other osmium NHC complexes. The hydride was located by the use of XHYDEX and was found to be bridging the Os(1)−Os(4) bond of 2.9049(6) Å length.[52] Other osmium−osmium bond lengths range from 2.6326(7) Å to 2.8569(6) Å.

An identical series of reactions must have occurred during thermolysis to form (**12**) as occurred to form (**11**) as previously discussed. The main difference between the formation of (**12**) and that of (**11**) is that the addition is regiospecific to accommodate the methyl group of toluene. Unfortunately, no mechanistic pathway can be deduced from the product structure.

Discrete single-site osmium carbyne complexes have also been reported, and these were formed from a triple benzylic dehydrogenation of cymene (4-isopropyltoluene) by an osmium amide complex.[92] Finally, metal-bound methyl groups have also been exhaustively dehydrogenated to give carbide complexes.[92]

The remarkable feature present in all these clusters is the persistent stability of the osmium−carbene bond, which remained intact in some form while decomposition and activation reactions occurred around the complex. The activation of toluene and benzene suggests a general reaction for simple aromatic compounds of this type. Such studies are beneficial to understanding NHC decomposition reactions.

Conclusions

Recent studies of NHC ligands in cluster systems have yielded a stunning array of complexes with unique reactivity in a short period of time. The formation of complexes resulting from multiple C−H and C−N bond activation has provided valuable insight into the decomposition of NHC ligands and provides a stark contrast to the chemistry observed for the ubiquitous phosphine ligand.[30,41,44−46]

(92) Lee, J.-H.; Pink, M.; Caulton, K. G. *Organometallics* **2006**, *25*, 802–804.

The persistence of silver-containing complexes and chloride substitution in the triosmium complexes treated with [(IMes)AgCl] should stand as prime examples of the complex nature of these reagents as well as the potential pitfalls associated with NHC transfer reactions. While successful transfer can be achieved in the case of the tetranuclear osmium−NHC complexes, rigorous characterization is needed to confirm the identity of the resulting products.

The complex reactivity that has resulted from the thermolysis of an osmium−NHC complex, notably, the activation of reaction solvent and the conversion of the carbene to an abnormal mode of coordination, exemplify the potential of cluster species containing adjacent metal sites to react in concert. The formation of higher nuclearity clusters resulting from the addition of unsaturated metal fragments has revealed interesting results, for example, the apparent C−N activation of a 2,4,6-trimethylphenyl group. Finally, the persistence of the osmium−carbene bond in all of these reaction products is of note, given the existence of the abnormal carbene derivative seemingly being present at elevated temperatures.

The thermolysis reaction products, one of which appears to result from a series of reactions including (a) exhaustive dehydrogenation of an *ortho*-methyl group on IMes; (b) partial dehydrogenation of a solvent molecule; and (c) C−C bond forming reaction between the two fragments (solvent and cluster) suggests that NHCs can engage in complex reactions with the cluster. The activation of benzene and toluene used as solvents in this system is indicative of the type of complex behavior that can result from cluster species. Finally, with respect to our observation of hexaphenylbenzene, dehydrogenation of aromatic compounds by transition metal complexes can be unpredictable leading to polyphenyl aromatic compounds. This observation has implications for the use of clusters as dehydrogenation catalysts in new organic H_2 storage systems *vis-à-vis* over dehydrogenation.

In addition, the thermolysis reaction led to the generation of trace amounts of two clusters of higher nuclearity than the reactant. These clusters have been identified as $\{Os_5(\mu_5\text{-}C)(\mu\text{-}H)(CO)_{14}[\eta\text{-}C\text{-}\eta\text{-}NC_2H_2(Mes)]\}$ and $[Os_6(\mu\text{-}H)_4(\mu_5\text{-}C)(CO)_{15}(IMes)]$, both carbide-containing species. It should be noted that the attempted thermolysis of $[Os_4(\mu\text{-}H)_4(CO)_{10}(IMes)_2]$ under similar conditions resulted in the formation of at least two products, which could not be isolated.

It is clear from the structure of both (**4**) and (**10**) that the osmium cluster can closely interact with the IMes ligand. This close approach, during thermolysis and either through agostic M−H−C interactions or through the loss of a CO ligand, may result in the activation and dehydrogenation of more than one C−H bond. This type of multiple C−H bond activation is, to our knowledge, unprecedented in NHC complexes of single metal-containing molecules, but multiple C−H activations appear to be commonplace for metal carbonyl clusters.

The strong basicity of NHCs increases the electron density of the metal atoms to which they are attached, and this enhances the tendency of these metals to become involved in oxidative addition processes. A combination of these two factors (unsaturated and electron-rich metals) rationalizes the results presented. A consequence of this reactivity is the multiple oxidative addition/cleavage of very strong bonds, such as C−H (sp^3) and C−N (sp^2).

The results reported herein, when taken with those found by Cabeza et al. and Whittlesey et al., reveal the utility of ruthenium and osmium cluster species at generating a wide range of products with unusual coordination and reactivity when NHCs are engaged as ligands.[30,41,44−46]

Experimental Section

General Procedures and Materials. Care should be exercised when working with osmium carbonyls becaue of health and exposure risks.[93] Reactions were carried out under nitrogen using standard Schlenk techniques. Solvents were purified by distillation, with hydrocarbons being distilled over potassium and dichloromethane over calcium hydride. Solvents were stored under an atmosphere of nitrogen over type 3A molecular sieves. The term, hexanes refers to a mixture of hexane isomers. High-pressure reactions were carried out in a 200-mL Parr autoclave. Gases were supplied by Praxair: nitrogen was pp (prepurifed) grade and dried in a CaH_2 drying tube, and CO was medical grade. ^{13}CO (99%) was purchased from Sigma-Aldrich and was used as received.

NMR spectra were collected using a 500-MHz Varian Inova NMR spectrometer (operational frequencies of 499.77 MHz for ^1H experiments and 125.68 MHz for $^{13}C\{^1H\}$ experiments) at SFU and a Bruker Advance II 600 MHz NMR spectrometer (operational frequencies, ^1H, 600.13 MHz; ^{13}C, 150.90 MHz). ^1H and $^{13}C\{^1H\}$ spectra are referenced to the residual solvent peak of chloroform-*d* (set to 7.260 ppm for ^1H and 77.00 ppm for $^{13}C\{^1H\}$ spectra) or dichloromethane-d_2 (set to 5.320 ppm for ^1H and 54.00 ppm for $^{13}C\{^1H\}$ spectra).

Infrared spectra were collected using a Bomen MB-100 infrared spectrometer, and unless otherwise stated, data was collected *in situ* using hexanes or dichloromethane as a solvent over a range of 2300 cm^{-1} to 1900 cm^{-1}. The resolution of the IR instrument was set to 2 cm^{-1} or 1 cm^{-1}, as needed. Mass spectrometry data was collected using a Kratos Concept double-focusing mass spectrometer with a LSIMS source. Elemental analyses of the compounds synthesized was completed at the Simon Fraser University Microanalytical Laboratory and at Canadian Micro Analytical Service Ltd.

$[Os_3(\mu\text{-}H)_2(CO)_{10}]$, $[Os_3(CO)_{10}(CH_3CN)_2]$, [(IMes)AgCl], $[Os_4(\mu\text{-}H)_4(CO)_{12}]$, and $[Ru_4(\mu\text{-}H)_4(CO)_{12}]$ were prepared by literature methods.[49,94,95] Trimethylamine *N*-oxide was obtained commercially and sublimed overnight at 40 °C.

The XHYDEX program of A. G. Orpen (University of Bristol) was used to predict or confirm the location of the H ligand in some hydride transition metal clusters.[52]

X-ray Experimental. Crystals of (**1**)−(**6**) and (**9**)−(**12**) were mounted on a glass fiber. Data were collected on a Nonius Kappa-CCD area detector diffractometer with COLLECT (Nonius B.V., 1997−2002). The unit cell parameters were calculated and refined from the full data set. Crystal cell refinement and data reduction were carried out using HKL2000 DENZO-SMN (Otwinowski and Minor, 1997). The absorption correction was applied using HKL2000 DENZO-SMN (SCALEPACK).

The SHELXTL/PC V6.14 for Windows NT (Sheldrick, G.M., 2001) suite of programs was used to solve the structure by direct methods. Subsequent difference Fourier syntheses allowed the remaining atoms to be located. All of the remaining non-hydrogen atoms were refined with anisotropic thermal parameters. The hydrogen atom positions were calculated geometrically and were included as riding on their respective carbon atoms.

Crystals of (**8**) were mounted on a glass fiber. Data were collected on a Bruker Smart Apex II diffractometer equipped with a Molybdenum X-ray tube (50 kV, 30 mA). Data collection and reduction were performed using the Bruker Apex II software package. The unit cell parameters were calculated and refined from the full data set.

(93) Drake, S. R.; Loveday, P. A. *Inorg. Synth.* **1990**, *28*, 230–231.
(94) Kaesz, H. D.; Knox, S. A. R.; Koepke, J. W.; Saillant, R. B. *J. Chem. Soc. D.* **1971**, 477.
(95) Knox, S. A. R.; Koepke, J. W.; rews, M. A.; Kaesz, H. D. *J. Am. Chem. Soc.* **1975**, *97*, 3942–3947.

The structure was solved via direct methods (sir 92), with subsequent refinements in CRYSTALS.[96] All non-hydrogen atoms were refined with anisotropic thermal parameters. The hydrogen atom positions were calculated geometrically and were refined with a riding model on their respective carbon atoms. The hydride atom H(X) was located during refinement (Table 12).

Preparation of $[Os_3(\mu\text{-}H)(\mu\text{-}Cl)(CO)_9(IMes)]$ (1). To a Carius tube was added $[Os_3(\mu\text{-}H)_2(CO)_{10}]$ (160 mg, 0.19 mmol), [(IMes)AgCl] (84 mg, 0.19 mmol), CH_2Cl_2 (20 mL), and hexanes (30 mL). The reaction vessel was degassed three times by freeze−pump−thaw methods and the purple reaction mixture placed in an oil bath overnight at 60 °C. The following morning, the reaction vessel was removed from heat and the solution cooled to room temperature. The reaction vessel contained an orange-yellow solution, and a small amount of dark solid was present at the bottom of the vessel. The solvent was removed *in vacuo*, the remaining solid dissolved in a minimum of CH_2Cl_2, and applied to a silica gel column.

Elution with CH_2Cl_2/hexanes (3:7 v/v) afforded an orange-yellow band of $[Os_3(\mu\text{-}H)(\mu\text{-}Cl)(CO)_9(IMes)]$, (**1**). The resulting solid was recrystallized from hexanes/toluene to afford (**1**) as orange-red crystals (41 mg, 19% yield). Other bands were also eluted, and these corresponded to $[Os_3(\mu\text{-}H)_2(CO)_{10}]$ and $[Os_3(CO)_{12}]$ as determined by infrared spectroscopy.[95,97]

Compound (**1**): IR (in hexanes) ν(CO): 2093 (m), 2051 (s), 2012 (vs), 2008 (sh,s), 2002 (s), 1990 (w), 1976 (m), 1971(m), 1939 (m) cm^{-1}. ^1H NMR (500 MHz, 295 K, CD_2Cl_2) δ −13.28 [s, 1H, μ-H], 2.10 [s, 6H, *ortho*-CH_3], 2.12 [s, 6H, *ortho*-CH_3], 2.36 [s, 6H, *para*-CH_3], 7.05 [s, 2H, *meta*-H], 7.07 [s, 2H, *meta*-H], 7.14 [s, 2H, *im*-H]. $^{13}C\{^1H\}$ NMR (125.61 MHz, 298 K, CD_2Cl_2) δ 18.6 [s, *ortho*-CH_3], 19.0 [s, *ortho*-CH_3] 21.4 [s, *para*-CH_3], 124.2 [s, N*CC*], 129.7 [s, Ar-*C*-3,5], 130.4 [s, Ar-*C*-3,5], 136.3 [s, Ar-*C*-2,6], 136.6 [s, Ar-*C*-2,6] 137.7 [s, Ar-*C*1,], 140.2 [s, Ar-*C*-4], 172.2 (s, 1C), 176.3 [s, carbene-*C*], 176.9 [s, 1C], 178.1 [s, 1C] 178.2 [s, 1C], 179.8 [s, 1C], 182.8 [s, 1C], 183.9 [s, 1C], 185.4 [s, 1C]. MS (LSIMS) *m*/*z* 1164.1 (M^+) (calcd. for M^+ 1164 (100%)). Anal. Calc. for $C_{30}H_{25}ClN_2O_9Os_3$: C, 30.96; H, 2.17; N, 2.41. Found: C, 30.93; H, 2.14; N, 2.47.

Preparation of $[Os_3(\mu\text{-}Cl)(CO)_{10}(\mu\text{-}Ag(IMes)]$ (2) and $[(IMes\text{-}H)][Os_3(\mu\text{-}Cl)(CO)_{10}](\mu_4\text{-}Ag)[Os_3(\mu\text{-}Cl)(CO)_{10}]$ (3). To a Schlenk tube was added $[Os_3(CO)_{10}(CH_3CN)_2]$ (101 mg, 0.11 mmol), [(IMes)AgCl] (49 mg, 0.11 mmol), and dry CH_2Cl_2 (30 mL). The resulting reaction mixture was allowed to stir at room temperature for 2 h. The reaction progress was followed by IR spectroscopy along with the disappearance of bands in the CO stretching region associated with $[Os_3(CO)_{10}(CH_3CN)_2]$, specifically 2023 cm^{-1}. An orange-red solution resulted. The solvent was removed under vacuum, the resulting solid dissolved in a minimum of CH_2Cl_2, and applied to a silica gel column. Elution with hexanes/CH_2Cl_2 afforded two bands. An orange band eluted with CH_2Cl_2/hexanes (1:4). The solvent was removed, and the resulting solid was recrystallized from hexanes to afford (**2**) as red crystals (49 mg, 35% yield). A second deep red band eluted with 100% dichloromethane, the solvent was removed, and the resulting solid was recrystallized from dichloromethane to afford $[(IMes\text{-}H)][Os_3(\mu\text{-}Cl)(CO)_{10}](\mu_4\text{-}Ag)[Os_3(\mu\text{-}Cl)(CO)_{10}]$ (**3**), as scarlet crystals (15 mg, 13% yield).

Compound (**2**): IR (in hexanes) ν(CO): 2092 (w), 2036 (vs), 2010 (s), 2003 (m), 1981 (w), 1974 (m), 1951 (m) cm^{-1}. ^1H NMR (400 MHz, 295 K, $CDCl_3$) δ 1.83 [s, 12, *ortho*-CH_3], 2.11 [s, 6H, *para*-CH_3], 6.76 [s, 4H, *meta*-H], 6.89 [d, 2H, *im*-H]. $^{13}C\{^1H\}$ NMR (100.61 MHz, 295 K, CD_2Cl_2) δ 17.6 [s, *ortho*-CH_3], 21.4 [s, *para*-CH_3], 122.6 [d, N*CC*], 129.8 [s, Ar-*C*-3,5], 134.9 [s, Ar-*C*-2,6], 135.4 [s, Ar-*C*1,], 139.7 [s, Ar-*C*-4], 173.4 [d, 2C], 178.2 [s, 2C], 181.4 [s 2C], 181.6 [s, 2C], 185.1 [t, 1C], 185.6 [t, 1C]. MS (LSIMS) *m*/*z* 1297.8 (M^+) (calcd for M^+ = 1300 (100%), 1299 (83%), 1298 (97%)). Anal. Calc. for $C_{31}H_{26}ClAgN_2O_{10}Os_3$: C, 28.63; H, 2.02; N, 2.15. Found: C, 28.40; H, 1.94; N, 2.01.

Compound (**3**): IR (in CH_2Cl_2) ν(CO): 2095.5 (w), 2085 (m), 2037 (br,s), 2032 (sh), 2000 (br,m), 1976(m,sh), 1959(br,m) cm^{-1}. ^1H NMR (500 MHz, 295 K, CD_2Cl_2) δ 2.14 [s, 12H, *ortho*-CH_3], 2.41 [s, 6H, *para*-CH_3], 7.16 [s, 4H, *meta*-H], 7.55 [d, 2H, *im*-H], 8.25 [s, C^+-H]. $^{13}C\{^1H\}$ NMR (100.61 MHz, 295 K, CD_2Cl_2) δ 17.7 [s, *ortho*-CH_3], 21.5 [s, *para*-CH_3], 125.7 [s, N*CC*], 130.8 [s, Ar-*C*-3,5], 134.4 [s, *C*1], 136.1 [s, Ar-*C*-2,6],136.9 [s, Ar-*C*1,], 143.3 [s, Ar-*C*-4], 175.3 [d, 2C], 179.5 [s, 2C], 183.5 [s, 2C], 185.0 [t, 1C], 185.3 [s, 2C], 186.0 [t, 1C]. MS (LSIMS) *m*/*z* 1883.4 (M^+) (calcd. M^+ = 1881 (100%), 1882 (92.9%), 1883 (92.3%)). Anal. Calc. for $C_{41}H_{25}AgCl_2N_2O_{20}Os_6$: C, 22.53; H, 1.15; N, 1.28. Found: C, 22.56; H, 1.20; N, 1.40.

Preparation of $[Os_4(\mu\text{-}H)_4(CO)_{11}(n\cdot IMes)]$ (4). $[Os_4(\mu\text{-}H)_4(CO)_{12}]$ (110 mg, 0.1 mmol) in CH_2Cl_2 (50 mL) was stirred with two equivalents of trimethylamine *N*-oxide (15 mg, 0.2 mmol) in CH_2Cl_2 (20 mL), being added dropwise over 20 min at 22 °C.[67,98] Subsequently, [(IMes)AgCl] (47.1 mg, 0.1 mmol) was added. After stirring for 2 h, the solution had changed color from yellow to dark orange-brown. The appearance of gray AgCl(s) in the bottom of the reaction vessel was used to determine reaction completion. The solvent was removed *in vacuo*, the remaining solid dissolved in a minimum of CH_2Cl_2, and applied to a silica gel column. Elution with CH_2Cl_2/hexanes (1:4) afforded a orange-yellow band of $[Os_4(\mu\text{-}H)_4(CO)_{11}(n\cdot IMes)]$ (**4**), (29 mg, 21%) and a second band corresponding to $[Os_4(\mu\text{-}H)_4(CO)_{11}(NMe_3)]$, a known compound.

Compound (**4**): IR (in CH_2Cl_2) ν(CO): 2094 (sh), 2085 (m), 2064 (sh), 2053 (vs), 2045 (s), 2023 (s), 1996 (m,br), 1979 (m), 1951 (w) cm^{-1}. ^1H NMR (500 MHz, 295 K, CD_2Cl_2) δ −20.14 [s,br, μ-H], 2.12 [s, 12H, *ortho*-CH_3], 2.35 [s, 6H, *para*-CH_3], 7.05 [s, 4H, *meta*-H], 7.09 [d, 2H, *im*-H]. $^{13}C\{^1H\}$ NMR (150.9 MHz, 295 K, CD_2Cl_2) δ 19.4 [s, *o*-CH_3], 21.4 [s, *p*-CH_3], 124.9 [s, *NCC*], 130.5 [s, *Ar*−*C*-3,5], 135.9 [s, *Ar*−*C*-2,6], 137.1 [s, *Ar*−*C1*,], 141.0 [s, *Ar*−*C*-*4*], 166.6 [s, 3C], 168.9 [br,s, 1C], 171.8 [s, 4C], 174.6 [br,s, 3C], 177.3 [s, 3C]. $^{13}C\{^1H\}$ NMR (150.9 MHz, 278 K, CD_2Cl_2) δ 166.6 [s, 2C], 169.3 [br,s, 1C], 171.6 [s, 3C], 175.6 [br,s, 2C], 177.3 [s, 3C]. MS (LSIMS) *m*/*z* 1377.9 (M^+) (calcd for M^+ = 1378 (100%)). Anal. Calc. for $C_{32}H_{28}N_2O_{11}Os_4$ C, 27.90, H 2.05, N 2.03. Found C, 27.77, H, 2.10, N 1.93.

Preparation of $[Os_4(\mu\text{-}H)_4(CO)_{10}(IMes)_2]$ (5) and $[Os_4(\mu\text{-}H)_3(\mu\text{-}Cl)(CO)_{11}(IMes)]$ (6). $[Os_4(\mu\text{-}H)_4(CO)_{12}]$ (110 mg, 0.1 mmol) in CH_3CN (50 mL) was stirred with trimethylamine *N*-oxide $(CH_3)_3NO$ (15 mg, 0.2mmol) in CH_3CN (20 mL), being added dropwise over 20 min at 22 °C. The solution was allowed to stir for approximately 2 h until the IR bands for $[Os_4(\mu\text{-}H)_4(CO)_{10}(CH_3CN)_2]$ were found to dominate. The reaction solution was filtered through a silica gel plug over a glass frit to remove any unreacted $[Os_4(\mu\text{-}H)_4(CO)_{12}]$ and $(CH_3)_3NO$. Literature preparations report a 90% yield for this initial step.[72] Because of the reactive nature of $[Os_4(\mu\text{-}H)_4(CO)_{10}(CH_3CN)_2]$, it was used *in situ* without further characterization or isolation.[72] The reaction mixture was concentrated down to about 20 mL under vacuum and transferred to a Carius tube fitted with a stir bar and a Teflon valve. An excess of [(IMes)AgCl] (160 mg, 0.36 mmol) was added to the reaction vessel, which was then degassed three times by freeze−pump−thaw methods and placed in an oil bath at 60 °C overnight. The solution changed color from yellow to dark orange-brown. The appearance of what appeared to be gray $AgCl_{(s)}$ in the bottom of the reaction vessel was used to determine reaction completion. The reaction vessel was cooled to room temperature, and the mixture was transferred to a Schlenk tube and the remaining solvent removed under vacuum. The remaining solid was redis-

(96) Betteridge, P. W.; Carruthers, J. R.; Cooper, R. I.; Watkin, D. J. *J. Appl. Crystallogr.* **2003**, *36*, 1487.

(97) Nicholls, J. N.; Vargas, M. D. Inorganic Synthesis; John Wiley & Sons, Inc.: New York, 1990; Vol. 28, pp 232−235.

(98) Li, Y.; Wong, W.-T. *J. Cluster Sci.* **2001**, *12*, 595–617.

Table 12

	compound				
	1	**2**	**3**	**4**	**5**
empirical formula	$C_{30}H_{25}ClN_2O_9Os_3 \cdot C_{3.5}H_4$	$C_{31}H_{24}AgClN_2O_{10}Os_3$	$C_{41}H_{25}AgCl_2N2O_{20}Os_6$	$C_{32}H_{28}N_2O_{11}Os_4$	$C_{52}H_{52}N_4O_{10}Os_4 \cdot C_{0.4}H_{0.8}Cl_{0.80}$
formula weight(g mol^{-1})	1209.64	1298.44	2185.60	1377.36	1687.75
temperature (K)	100(2)	150(2)	296(2)	150(2)	296(2)
λ(Mo Kα) (Å)	0.71073	0.71073	0.71073	0.71073	0.71073
crystal system	triclinic	triclinic	monoclinic	orthorhombic	monoclinic
space group	$P\bar{1}$	$P\bar{1}$	*C*2/*c*	*P*ca2(1)	*P*2(1)/n
a(Å)	8.3651(2)	8.1388(6)	14.5755(8)	27.9147(5)	10.2720(3)
b (Å)	10.8743(3)	12.5307(9)	21.6908(16)	16.5133(3)	22.8096(5)
c (Å)	20.4975(7)	18.0480(10)	17.6188(11)	15.2219(2)	24.0937(5)
α (°)	80.968(2)	93.746(4)	90	90	90
β (°)	81.369(2)	97.217(4)	106.714(3)	90	94.1310(10)
γ (°)	71.935(2)	97.567(3)	90	90	90
volume ($Å^3$), *Z*	1740.42(9), 2	1803.9(2), 2	5334.9(6),4	7016.7(2), 8	5630.5(2), 4
ρ (calculated, Mg m^{-3})	2.308	2.391	2.271	2.608	1.991
μ (mm^{-1})	11.056	11.195	14.763	14.500	9.092
F(000)	1122	1192	3928	5008	3171
crystal size (mm)	0.22 × 0.17 × 0.13	0.28 × 0.15 × 0.08	0.30 × 0.28 × 0.10	0.10 × 0.07 × 0.08	0.20 × 0.10 × 0.05
θ Range (°)	2.58 to 26.37	2.55 to 25.03	2.61 to 23.25	2.57 to 25.03	2.67 to 25.03
index ranges	−10 to 10, −13 to 13, −25 to 25	−9 to 9, −14 to 14, −21 to 21	−16 to 16, −24 to 22, −19 to 19	−33 to33, −19 to 19,−18 to 18	−12 to 12, −27 to 27, −28 to 28
number of reflections collected	21096	17458	14906	70738	55539
number of independent reflections	7106,[R_{int} = 0.054]	6323,[R_{int} = 0.095]	3610,[R_{int} = 0.0678]	12020,[R_{int} = 0.129]	9942,[R_{int} = 0.107]
goodness-of-fit on F^2	1.034	0.944	1.007	0.969	1.022
final *R* indices	*R*1 = 0.0344,*wR*2 = 0.0822	*R*1 = 0.0540,*wR*2 = 0.1009	*R*1 = 0.0669,*wR*2 = 0.1610	*R*1 = 0.0478,*wR*2 = 0.0902	*R*1 = 0.0495,*wR*2 = 0.1192
R indices (all data)	*R*1 = 0.0441,*wR*2 = 0.0856	*R*1 = 0.1154,*wR*2 = 0.1196	*R*1 = 0.1147, *wR*2 = 0.1855	*R*1 = 0.0839,*wR*2 = 0.1011	*R*1 = 0.0854,*wR*2 = 0.1343
largest diff peak hole (e.$Å^{-3}$)	1.952/−2.350	1.746/−2.501	2.457/−2.372	2.221/−2.559	1.371/−1.612

	compound					
6	**8**	**9**	**10**	**11**	**12**
$C_{32}H_{27}ClN_2O_{11}Os_4$	$C_{27}H_{14}N_2O_{14}Os_5$	$C_{37}H_{28}O_{15}Os_6$	$C_{32}H_{28}N_2O_{11}Os_4$	$C_{40}H_{33}N_2O_{10}Os_4 \cdot C_3H_7$	$C_{38}H_{28}N_2O_{10}Os_4 \cdot C_{0.5}HCl$
1411.81	1541.41	1881.81	1377.36	1462.48	1475.89
150(2)	293	150(2)	150(2)	150(2)	150(2)
0.71073	0.71073	0.71073	0.71073	0.71073	0.71073
orthorhombic	monoclinic	monoclinic	triclinic	triclinic	triclinic
*P*na21	*P* 1 21/n 1	*P*2(1)/n	$P\bar{1}$	$P\bar{1}$	$P\bar{1}$
24.1236(13)	17.8450(15)	10.4402(2)	14.0262(5)	12.3074(4)	12.03075(5)
11.6068(6)	10.7365(9)	24.0703(6)	15.9043(6)	12.6819(4)	12.7131(7)
31.1183(17)	19.3626(16)	17.0669(4)	16.2286(6)	14.7598(5)	15.1134(7)
90	90	90	96.672(2)	74.792(2)	73.738(2)
90	116.698(4)	104.1130(10)	96.046(2)	87.235(2)	86.774(3)
90	90	90	90.049(2)	62.317(2)	62.890(2)
8713.1(8),8	3314.2(5), 4	4159.44(16), 4	3575.4(2), 4	1961.26(11), 2	2013.67(17), 2
2.153	3.089	3.005	2.559	2.476	2.434
11.740	19.167	18.326	14.229	12.976	12.704
5136	2728	3360	2504	1342	1350
0.40 × 0.30 × 0.03	0.046 × 0.110 × 0.123	0.13 × 0.08 × 0.05	0.35 × 0.25 × 0.05	0.40 × 0.17 × 0.04	0.50 × 0.33 × 0.26
2.62 to 23.26	2.090 to 36.224	2.60 to 25.02	2.71 to 25.03	2.61 to 25.03	2.62 to 25.03
−26 to 26, −12 to 12, −34 to 34	−29 to 29, −16 to 17, −30 to −29	−12 to 12, −28 to 28, −20 to 20	−16 to 16, −18 to 18, −19 to 18	−14 to 14, −14 to 15, −17 to 17	−14 to 14, −14 to 15, −17 to 17
69533	117814	46405	37795	22185	24599
12292,[R_{int} = 0.086]	15182,[R_{int} = 0.073]	7334,[R_{int} = 0.094]	12034,[R_{int} = 0.69]	6620,[R_{int} = 0.057]	7057,[R_{int} = 0.0870]
1.048	0.6095	1.039	1.020	1.040	0.881
*R*1 = 0.0736,*wR*2 = 0.2010	*R*1 = 0.0314, *wR*2 = 0.0354	*R*1 = 0.0464,*wR*2 = 0.1174	*R*1 = 0.0672, *wR*2 = 0.1781	*R*1 = 0.0513, *wR*2 = 0.1408	*R*1 = 0.0411, *wR*2 = 0.0579
*R*1 = 0.0874,*wR*2 = 0.2146	*R*1 = 0.0852, *wR*2 = 0.0576	*R*1 = 0.0645, *wR*2 = 0.1268	*R*1= 0.0750, *wR*2= 0.1878	*R*1 = 0.0552, *wR*2 = 0.1448	*R*1 = 0.1143, *wR*2 = 0.0713
3.805/−3.421	4.46/−2.42	2.482/−2.458	7.890/−4.527	6.134/−3.193	1.334/−1.551

solved in a minimum amount of CH_2Cl_2 and applied to a silica gel column. From multiple preparations, it was found that the orange band, which appeared on the column, if left alone would change color to green, decomposing on the column. Application of CH_2Cl_2/hexanes (3:7) under high nitrogen gas pressure allowed for elution of the green decomposition material. This was followed by rapid elution with CH_2Cl_2/hexanes (3:2), which afforded an orange band of $[Os_4(\mu\text{-}H)_4(CO)_{10}(IMes)_2]$ (**5**) (74 mg, 45%).

Trailing on the column was another green band, which was collected by elution with dichloromethane. Upon leaving the eluted green solutions to stir overnight, it was found that they continued to decompose, resulting in orange solutions the following morning.

IR studies of this solution revealed a complex set of bands in the ν(CO) region, suggesting that a mixture of compounds was present in both samples, which were subsequently combined. The solvent was removed under vacuum, the residue redissolved in a minimum amount of CH_2Cl_2, and applied to a silica gel column. Elution with CH_2Cl_2/hexanes (1:4) afforded four bands: first, $[Os_3(\mu\text{-H})(\mu\text{-Cl})(CO)_9(IMes)]$ (**1**); second, the previously prepared $[Os_4(\mu\text{-H})_4(CO)_{11}(IMes)]$ (**4**); third, $[Os_4(\mu\text{-H})_4(CO)_{12}]$, the parent osmium hydride compound; and finally, the new cluster $[Os_4(\mu\text{-H})_3(\mu\text{-Cl})(CO)_{11}(IMes)]$ (**6**) (13 mg, 9%). The structures of the previously characterized compounds (**1**) and (**4**) were confirmed by IR and NMR spectroscopic methods.

Compound (**5**): IR (in CH_2Cl_2) ν(CO): 2059 (m), 2034 (s), 2013 (vs), 1981 (s), 1967 (m), 1943 (m), 1922 (w) cm^{-1}. ^1H NMR (600 MHz, 298 K, CD_2Cl_2) δ −21.81 [s, 1H μ-H], −21.77 [s, 1H μ-H],−19.36 [s, 1H μ-H], −18.68 [s, 1H μ-H], 1.95 [s, 6H, *ortho*-CH_3], 2.03 [s, 6H, *ortho*-CH_3], 2.04 [s, 6H, *ortho*-CH_3], 2.14 [s, 6H, *ortho*-CH_3] 2.29 [s, 6H, *para*-CH_3], 2.36 [s, 6H, *para*-CH_3], 6.88 [br,s, 2H, *meta*-H], 6.96 [br,s, 2H, *meta*-H], 6.99 [s, 2H, *im*-H], 7.00 [br,s, 2H, *meta*-H], 7.01 [s, 2H, *im*-H], 7.02 [br,s, 2H, *meta*-H]. $^{13}C\{^1H\}$ NMR (150.95 MHz, 290 K, $CDCl_2$) δ 18.8 [s, *o*-CH_3], 19.2 [s, *o*-CH_3], 19.5 [s, *o*-CH_3], 19.7 [s, *o*-CH_3], 21.3 [s, *p*-CH_3], 21.47 [s, *p*-CH_3], 124.1 [s, N*CC*], 124.6 [s, N*CC*], 129.5 [s, Ar-*C*-3,5], 130.1 [s, Ar-*C*-3,5], 130.2 [s, Ar-*C*-3,5], 130.5 [s, Ar-*C*-3,5], 135.5 [s, Ar-*C*-2,6], 136.0 [s, Ar-*C*-2,6], 136.3 [s, Ar-*C*-2,6], 136.4 [s, Ar-*C*-2,6], 137.2 [s, Ar-*C*1,], 138.2 [s, Ar-*C*1,], 139.1 [s, Ar-*C*-4]. 140.4 [s, Ar-*C*-4]. $^{13}C\{^1H\}$ NMR (150.95 MHz, 298 K, $CDCl_2$) δ 164.3 [s, 1C], 171.2 [s, 1C], 173.0 [s, 1C], 173.0 [br,s, 1C], 175.2 [br,s, 1C], 177.9 [br,s], 178.3 [br,s], 178.9 [br, s], 179.7 [br, s], 181.4 [br,s], 182.6 [br,s], 183.0 [br,s], 183.5 [br,s]. ^{13}C NMR (150.95 MHz, 298 K, $CDCl_2$) δ 164.3 [d, J_{CH} = 7.8 Hz, 1C], 171.2 [d, J_{CH} = 7.7 Hz, 1C], 173.0 [d, J_{CH} = 4.4 Hz, 1C], 173.0 [br,s, 1C], 175.2 [br,s, 1C], 177.9 [br,s], 178.3 [br,s], 178.9 [br,s], 179.7 [br,s], 181.4 [br,s], 182.6 [br,s], 183.0 [br,s], 183.5 [br,s]. MS (LSIMS) *m/z* 1654.0 (M^+) (calcd. M^+ = 1654 (100%)). Anal. Calc. for $C_{52}H_{52}N_4O_{10}Os_4$ C, 37.76, H 3.17, N 3.39. Found C, 37.14, H, 3.14, N, 3.12.

Compound (**6**): IR (in CH_2Cl_2) ν(CO): 2087 (m), 2060 (vs), 2043 (s), 2022 (s), 1995 (m), 1977 (m), 1948 (br,m) cm^{-1}. ^1H NMR (600 MHz, 298 K, CD_2Cl_2) δ −18.41 [s, 1H μ-H], −12.64 [s, 2H μ-H], 2.24 [s, 12H, *ortho*-CH_3], 2.29 [s, 6H, *para*-CH_3], 7.05 [s, 4H, *meta*-H], 7.19 [s, 2H, im-H]. $^{13}C\{^1H\}$ NMR (150.95 MHz, 298 K, CD_2Cl_2) δ 18.6 [s, *o*-CH_3], 21.5 [s, *p*-CH_3], 125.8 [s, N*CC*], 130.5 [s, Ar-*C*-3,5], 136.3 [s, Ar-*C*-2,6], 137.7 [s, Ar-*C*1,], 141.9 [s, Ar-*C*-4]. 150.7 [t, carbene-*C*], 171.1 [dd, $J_{CH(cis)}$ = 2.9 Hz, $J_{CH(trans)}$ = 11.3 Hz 2C], 174.6 [s, 2C], 178.0 [s, 2C], 178.8 [br,s, 1C], 180.5 [d, $J_{CH(trans)}$ = 11.6 Hz, 2C], 182.3 [s, 2C]. MS (LSIMS) *m/z* 1412.00 (M^+) (calcd. M^+ = 1412 (100%)). Anal. Calc. for $C_{32}H_{27}N_2O_{10}Os_4$ C, 27.22, H 1.93, N 1.98. Found C, 30.57, H, 2.41, N, 1.95.

Preparation of $[Ru_4(\mu\text{-H})_4(CO)_{11}(IMes)]$ (7). $[Ru_4(\mu\text{-H})_4(CO)_{12}]$ (0.140 mg, 0.2 mmol) in CH_2Cl_2 (30 mL) was stirred with two equivalents of trimethylamine *N*-oxide (28 mg, 0.4 mmol) in CH_2Cl_2 (20 mL), being added dropwise over 20 min at 22 °C.[98] Subsequently, [(IMes)AgCl] (47.1 mg, 0.1mmol) was added. After stirring for 1 h, the solution had changed color from yellow to dark orange-brown. The appearance of a fine gray powder believed to be AgCl(s) in the bottom of the reaction vessel was used to determine reaction completion. The solvent was removed *in vacuo*, the remaining solid dissolved in a minimum volume of CH_2Cl_2, and applied to a silica gel column. Elution with CH_2Cl_2/hexanes (1:4) afforded a single orange-yellow band of $[Ru_4(\mu\text{-H})_4(CO)_{11}(IMes)]$ (**7**), (65 mg, 34%). When left at ambient temperature in air or nitrogen for extended periods of time, the complex decomposed.

Compound (**7**): IR (in hexanes) ν(CO): 2083 (m), 2063(w), 2048 (vs), 2028 (s), 2002 (m), 1986 (m), 1967 (br,w), 1954 (w) cm^{-1}. ^1H NMR (600 MHz, 295 K, CD_2Cl_2) δ −18.0 [br,s, 2H μ-H], −17.8 [br,s, 2H μ-H], 2.10 [s, 12H, *ortho*-CH_3], 2.35 [s, 6H, *para*-CH_3], 7.05 [s, 4H, *meta*-H], 7.09 [d, 2H, *im*-H]. $^{13}C\{^1H\}$ NMR (150.90 MHz, 295 K, CD_2Cl_2) δ 19.0 [s, *o*-CH_3], 21.4 [s, *p*-CH_3], 125.0 [s, *NCC*], 130.4 [s, *Ar*−*C*-3,5], 135.9 [s, *Ar*−*C*-2,6], 137.3 [s, *Ar*−*C1*,], 172.2 [s, Carbene-*C*], 188.6 [s, 2C], 195.0 [br,s, 7C], 198.2 [s, 3C]. MS (LSIMS) (calcd for M^+ = 1022 (100%)). Anal. Calc. for $C_{32}H_{28}N_2O_{11}Ru_4$ C, 37.65, H 2.76, N 2.74. Found C, 37.64, H, 2.77, N 2.63.

Preparation of $\{Os_5(\mu_5\text{-C})(\mu\text{-H})(CO)_{14}[\eta\text{-C-}\eta NC_2H_2(Mes)]\}$ (8), $[Os_6(\mu\text{-H})_4(\mu_5\text{-C})(CO)_{15}(IMes)]$ (9), $[Os_4(\mu\text{-H})_4(CO)_{11}(a\cdot IMes)]$ (10), and $\{Os_4(\mu\text{-H})(CO)_{10}[\eta\text{-C})N(Mes)C_2H_2NC_6H_2(CH_3)_2(\eta^2\text{-C})(\eta\text{-C})\text{-}C_4H_4(\eta^2\text{-C})]\}$ (11). $[Os_4(\mu\text{-H})_4(CO)_{11}(n\cdot IMes)]$ (184 mg, 0.133 mmol) was dissolved in benzene (15 mL) and heated to 200 °C in a Carius tube degassed three times by freeze−pump−thaw techniques. After 48 h, the solution was cooled and the solvent removed *in vacuo*. The remaining solid was dissolved in a minimum of CH_2Cl_2 and applied to a silica gel column. IR spectroscopic studies were performed on the reaction mixtures before and after column chromatography, and these studies indicated that no rearrangements occurred on the column. $\{Os_5(\mu_5\text{-C})(\mu\text{-H})(CO)_{14}[\eta\text{-C-}\eta\text{-}NC_2H_2\text{-(Mes)}]\}$ (**8**) was eluted with CH_2Cl_2/hexanes (1:4) as a very pale yellow band (10 mg, 6%). This was followed by a yellow band of $[Os_4(\mu\text{-H})_4(CO)_{11}(a\cdot IMes)]$ (**10**), (63 mg, 34%). $\{Os_4(\mu\text{-H})(CO)_{10}[(\eta\text{-C})N(Mes)C_2H_2NC_6H_2(CH_3)_2(\eta^2\text{-C})(\eta\text{-C})C_4H_4(\eta^2\text{-C})]\}$ (**11**) was eluted with CH_2Cl_2/hexanes (1:4) as a red-brown band (31 mg, 16%). Lastly, elution with CH_2Cl_2/hexanes (1:4) gave an orange-red band of $[Os_6(\mu\text{-H})_4(\mu_5\text{-C})(CO)_{15}(IMes)]$ (**9**) (11 mg, 7%).

Compound (**8**): IR (in CH_2Cl_2) ν(CO): 2106 (m), 2078 (s), 2057 (vs), 2025 (m), 2007 (s), 1990 (br,m), 1975 (sh,w), 1946 (br,w) cm^{-1}. ^1H NMR (500 MHz, 295 K, CD_2Cl_2) δ 1.79 [s, 6H, *o*-CH_3], 2.34 [s, 3H, *p*-CH_3], 6.31 [s, 1H, η-N-C-*im*-H], 6.96 [s, 2H, *meta*-H], 7.04 [s, 1H, *im*-H]. $^{13}C\{^1H\}$ NMR (150.92 MHz, 295 K, CD_2Cl_2) δ 18.6 [s, *o*-CH_3], 21.4 [s, *p*-CH_3], 122.1 [s, *NCC*], 129.5 [s, *Ar*−*C*-3,5], 132.4 [s, η-*NCC*], 136.1 [s, *Ar*−*C*-2,6], 137.8 [s, *Ar*−*C1*], 139.5 [s, *Ar*−*C-4*]. 160.7 [1C], 170.5 [2C], 172.2 [2C], 173.3 [2C], 173.9 [2C], 174.5 [1C], 176.7 [2C], 181.2 [2C], 377.9 [s, μ_5-C]. MS (LSIMS) *m/z* 1541.6 (M^+) (calcd for M^+ = 1541 (91.8%), 1542 (100%). Anal. Calc. for $C_{27}H_{14}N_2O_{14}Os_5$ C, 21.04, H 0.92, N 1.82. Found C, 21.10, H, 0.86, N 1.72.

Compound (**9**): IR (in CH_2Cl_2) ν(CO): 2088 (m), 2055 (s), 2043 (vs), 2018 (s), 2011 (s), 1996 (m), 1947 (br,w) cm^{-1}. ^1H NMR (600 MHz, 295 K, CD_2Cl_2) δ −9.85 [s, 1H, μ-H], −9.84 [s, 1H, μ-H], −9.80 [s, 1H, μ-H], −9.79 [s, 1H, μ-H], 2.14 [s, 3H, *o*-CH_3], 2.22 [s, 3H, *o*-CH_3], 2.26 [s, 3H, *o*-CH_3], 2.36 [s, 3H, *o*-CH_3], 2.40 [s, 3H, *p*-CH_3] 2.50 [s, 3H, *p*-CH_3], 7.13 [s, 1H, *meta*-H], 7.22 [s, 1H, *meta*-H], 7.13 [s, 1H, *meta*-H], 7.13 [s, 1H, *meta*-H], 7.25 [d, J_{HH} = 2 Hz, 1H, *im*-H], 7.37 [d, J_{HH} = 2 Hz, 1H, *im*-H], 7.30 [s, 1H, *meta*-H]. $^{13}C\{^1H\}$ NMR (150.92 MHz, 295 K, CD_2Cl_2) δ 18.8 [s, *o*-CH_3], 19.2 [s, *o*-CH_3], 19.4 [s, *o*-CH_3], 19.8 [s, *o*-CH_3], 21.5 [s, *p*-CH_3], 21.6 [s, *p*-CH_3], 124.7 [s, *NCC*], 125.8 [s, *NCC*], 129.0 [s, *Ar*−*C*-3], 129.2 [s, *Ar*−*C*-3], 130.5 [s, *Ar*−*C*-5], 130.7 [s, *Ar*−*C*-5], 136.2 [s, *Ar*−*C-2*], 136.3 [s, *Ar*−*C*-2], 136.6 [s, *Ar*−*C-6*], 136.6 [s, *Ar*−*C*-1], 137.0 [s, *Ar*−*C-4*], 137.5 [s, *Ar*−*C*-1], 141.6 [s, *Ar*−*C*-4], 142.0 [s, *Ar*−*C*-4], 171.4 [N*C*N], 173.5 [3C], 173.9 [2C], 174.1 [2C], 178.5 [2C], 178.6 [2C], 185.2 [2C], 186.6 [2C], 353.8 [s, μ_5-C]. MS (LSIMS) *m/z* 1881.8 (M^+) (calcd for M^+ = 1882 (100%). Anal. Calc. for $C_{37}H_{28}N_2O_{15}Os_6$ C, 23.61, H 1.50, N 1.49. Found C, 23.32, H, 1.27, N 1.39.

Compound (**10**): IR (in CH_2Cl_2) ν(CO): 2084 (m), 2052 (vs), 2038 (s), 2021 (s), 1995 (m), 1985 (m), 1977 (m), 1942 (sh,w) cm^{-1}. ^1H NMR (600 MHz, 295 K, CD_2Cl_2) δ −20.50 [s,1H,], −19.85 [s,2H, μ-H], −19.85 [s,1H, μ-H], 2.07 [s, 3H, *o*-CH_3], 2.09 [s, 3H, *o*-CH_3], 2.11 [s, 3H, *o*-CH_3], 2.2 [s,br, 3H, *o*-CH_3], 2.2 [s,br, 6H, *p*-CH_3], 6.63 [s, 1H, *meta*-H], 6.68 [s, 2H, *meta*-H], 7.04 [s, 1H, im-H], 7.07 [s, 1H, im-H], 7.09 [s, 2H, im-H], 7.95 [s, 2H, C(1)-H], 7.99 [s, 1H, C(1)-H]. $^{13}C\{^1H\}$ NMR (150.92 MHz, 298 K, CD_2Cl_2) δ 17.3 [s, *o*-CH_3], 17.4 [s, *o*-CH_3], 18.3 [s, *o*-CH_3],

21.4 [s, *p*-CH_3], 21.5 [s, *p*-CH_3], 126.0 [s, *NCa•NHC•C*], 129.9 [s, *Ar−C*-3,5], 130.1 [s, *Ar−C*-3,5], 130.2 [s, *Ar−C*-3,5], 131.4 [s, *Ar−C*-3,5], 134.1 [s, *Ar−C*-2,6], 134.2 [s, *Ar−C*-2,6], 134.4 [s, *Ar−C*-2,6], 134.7 [s, *Ar−C*-2,6] 135.0 [s, *Ar−C1*], 136.0 [s, *Ar−C1*,], 141.4 [s, *Ar−C-4*], 141.8 [s, N*C*CHN], 141.9 [s, *Ar−C-4*], 167.0 [br,s, 1C], 169.6 [sh, 1C], 170.4 [s, 1C], 171.0 [s, 1C], 171.5 [s, 1C], 171.9 [s, 1C], 176.8 [br,s, 1C], 177.4 [s, 2C], 177.8 [s, 1C]. $^{13}C\{^1H\}$ NMR (150.92 MHz, 273 K, CD_2Cl_2) δ 168.6 [br,s, 1C], 169.8 [br,s, 1C], 170.3 [s, 1C], 171.0 [s, 1C], 171.4 [s, 1C], 171.8 [s, 1C], 173.5 [br,s, 1C], 176.0 [br,s, 1C], 177.4 [s, 2C], 177.8 [s, 1C], 180.3 [br,s, 1C]. MS (LSIMS) *m/z* 1377.9 (M^+) (calcd for M^+ = 1378 (100%)). Anal. Calc. for $C_{32}H_{28}N_2O_{11}Os_4$ C, 27.90, H 2.05, N 2.03. Found C, 27.77, H, 1.94, N 1.79.

Compound (**11**): IR (in CH_2Cl_2) ν(CO): 2076 (s), 2044 (vs), 2013 (s), 1996 (s), 1980 (m), 1969 (m), 1916 (br,w) cm^{-1}. ^1H NMR (600 MHz, 295 K, CD_2Cl_2) δ −19.95 [s, μ-H], 1.32 [s, 3H, H57], 2.20 [s, 3H, H59], 2.30 [s, 3H, H58], 2.33 [s, 3H, H67], 2.59 [s, 3H, H68], 6.86 [m, 1H, H75A], 6.88 [s, 1H, H53A], 6.92 [s, 1H, H55A], 7.03 [s, 1H, H63A], 7.11 [s, 1H, H63A], 7.17 [d, J_{HH} = 2.3 Hz, 1H, H4A], 7.18 [m, 1H, H74A], 7.57 [d, J_{HH}= 8.7 Hz, 1H, H76A], 7.71 [d, J_{HH} = 2.3 Hz, 1H, H3A], 7.84 [d, J_{HH} = 7.8 Hz, 1H, H73A]. $^{13}C\{^1H\}$ NMR (150.91 MHz, 295K, CD_2Cl_2) δ 18.5 [s, C57], 19.7 [s, C59], 20.5 [s, C67], 21.0 [s, C68], 21.3 [s, C58], 120.6 [s, C53], 123.8 [s, C4], 123.9 [s, C3], 128.1 [s, C55], 129.3 [s, C75], 129.5 [s, C63], 130.0 [s, C76], 130.8 [s, C74], 131.1 [s, C73], 132.4 [s, C65], 134.3 [s, C52], 135.8 [s, C56], 135.9 [s, C62], 136.9 [s, C51], 137.0 [s, C61], 140.8 [s, C66], 147.0 [s, C54], 148.0 [s, C64], 155.2 [s, C69], 162.9 [s, C71], 166.6 [s, C72], 181.0 [s, C1]. MS (LSIMS) *m/z* 1419.7 (M^+) (calcd for M^+ = 1420 (100%)). Anal. Calc. for $C_{37}H_{26}N_2O_{10}Os_4$ C, 31.31, H 1.85, N 1.97. Found C 31.32, H 1.99, N 1.72.

Solution studies: (**10**) (45 mg, 0.033 mmol) was dissolved in benzene (20 mL) and heated to 200 °C in a Carius tube degassed three times by freeze−pump−thaw techniques. After 48 h, the reaction mixture was subjected to column chromatography and the isolated materials corresponded to (**11**) (23 mg, 0.016 mmol) and a trace of (**4**). Infrared spectroscopic evidence for the generation of a small amount of $[Os_4(\mu\text{-H})_4(CO)_{12}]$ was also observed as indicated by diagnostic bands at 2067 and 2019 cm^{-1}. Some insoluble black material was noted at the top of the column.

Preparation of {$Os_4(\mu$-H)$(CO)_{10}[\eta$-C)N(Mes)$C_2H_2NC_6H_2(CH_3)_2$-(η^2-C)(ηC)CHC$(CH_3)C_2H_2(\eta^2$-C)]} (12). $[Os_4(\mu\text{-H})_4(CO)_{11}$-($n$•IMes)] (110 mg, 0.200 mmol) was dissolved in toluene (15 mL) and heated to 200 °C in a Carius tube degassed three times by freeze−pump−thaw techniques. After 72 h, the solution was cooled and the solvent removed *in vacuo*. The remaining solid was dissolved in a minimum of CH_2Cl_2 and applied to a silica gel column. IR spectroscopic studies were performed on the reaction mixtures before and after column chromatography, and these studies indicated that no rearrangements occurred on the column. {$Os_5(\mu_5$-C)$(CO)_{14}[\eta$-C-η-NC_2H_2(Mes)]} (**8**) was eluted with CH_2Cl_2/hexanes (1:4) as a very pale yellow band (6 mg, 6%). This was followed by a yellow band of $[Os_4(\mu\text{-H})_4(CO)_{11}(a$•IMes)] (**10**), (13 mg, 12%). {$Os_4(\mu$-H)$(CO)_{10}[(\eta$-C)N(Mes)$C_2H_2NC_6H_2(CH_3)_2(\eta^2$-C)($\eta$-C)CHC$(CH_3)C_2H_2(\eta^2$-C)]} (**12**) was eluted with CH_2Cl_2/hexanes (1:4) as a red-brown band (25 mg, 22%). Lastly, elution with CH_2Cl_2/hexanes (1:4) gave an orange-red band of $Os_6(\mu\text{-H})_4(\mu_5$-C)$(CO)_{15}$(IMes)] (**9**), (5 mg, 5%).

Compound (**12**): IR (in CH_2Cl_2) ν(CO): 2075 (s), 2043 (vs), 2012 (s), 1995 (s), 1979 (m), 1968 (m), 1915 (br,w) cm^{-1}. ^1H NMR (600 MHz, 295 K, CD_2Cl_2) δ −19.98 [s, μ-H], −19.96 [s, μ-H], 1.32 [s, 3H, H57], 1.33 [s, 3H, H57], 2.09 [s, 3H, H78], 2.19 [s, 3H, H58], 2.29 [s, 3H, H67], 2.32 [s, 3H, H59], 2.33 [s, 3H, H59], 2.41 [s, 3H, H77], 2.59 [s, 3H, H68], 6.73 [d, J_{HH} = 8.5 Hz, 1H, H74A], 6.88 [s, H, H55A] 6.90 [s, 1H, H53A], 6.91 [s, 1H, H53A], 7.02 [s, 2H, H63A], 7.05 [d, J_{HH} = 8.9 Hz, H75A], 7.10 [s, 2H, H65A], 7.17 [d, J_{HH} = 5.1 Hz, H4A], 7.26 [s, 1H, H76A], 7.48 [d, J_{HH} = 8.8 Hz, H76A], 7.64 [s, 1H, H73A], 7.71 [d, J_{HH} = 5.1 Hz, 2H, H3A], 7.73 [d, J_{HH} = 8.5 Hz, H73A]. $^{13}C\{^1H\}$ NMR (150.91 MHz, 295K, CD_2Cl_2) 18.5 [s, C78], 19.8 [s, C57], 19.8 [s, C57], 20.4 [s, C59], 20.5 [s, C59], 20.9 [s, C58], 21.0 [s, C58], 21.3 [s, C77], 21.6 [s, C67], 21.9 [s, C68], 123.4 [s], 123.6 [s], 123.6 [s], 123.7 [s], 123.8 [s], 127.9 [s], 128.0 [s], 128.4 [s], 129.1 [s], 129.2 [s], 129.4 [s], 129.9 [s], 130.5 [s], 130.7 [s], 131.4 [s], 131.4 [s], 133.7 [s], 134.2 [s], 134.2 [s], 135.7 [s], 135.8 [s], 136.8 [s], 136.8 [s], 136.9 [s], 140.7 [s], 141.6 [s], 144.2 [s], 147.8 [s], 147.9 [s], 148.3 [s], 153.1 [s], 154.8 [s], 162.8 [s], 162.9 [s], 166.5 [s], 166.6 [s], 166.6 [s], 166.7 [s], 170.8 [s], 171.7 [s], 173.4 [s], 181.1 [br,s, 3C], 182.4 [s, 1C], 182.7 [s, 1C], 183.4 [s, 1C], 184.3 [s, 1C], 184.6 [s, 1C], 188.9 [s, 1C], 189.0 [s, 1C]. MS (LSIMS) *m/z* 1433.9 (M^+) (calcd for M^+ = 1435 (100%), 1434 (88.6%)). Anal. Calc. for $C_{38}H_{29}N_2O_{10}Os_4$ C, 31.84, H 1.97, N 1.95. Found C 32.01, H 2.22, N 2.09.

Acknowledgment. Funding was provided by the Natural Sciences and Engineering Council of Canada (NSERC) through the Discovery Grants Program to J.A.C.C. and R.K.P. J.A.C.C. acknowledges generous support from the Canada Research Chairs Program, the Canadian Foundation for Innovation, and the Nova Scotia Research and Innovation Trust Fund, and ARMRC for NMR acquisition.

Note Added in Proof. A recent paper reported in this journal described a DFT study on the double C-H bond activation of NHC *N*-Methyl substituents with Ru3 and Os3 carbonyl clusters (Cabeza, Javier A.; Perez-Carreno, E. *Organometallics* **2008**, *27*, 4697–4702.

Supporting Information Available: Crystallographic information files (CIF) of the complexes and selected spectra data are available. This material is also available free of charge via the Internet at http://pubs.acs.org.

OM800577X